THE Journal OF THE AMERICAN LEATHER CHEMISTS ASSOCIATION

April 2024 | Vol. CXIX, No.4 | *JALCA* 119(4), 153–204, 2024

Contents

Distributed by
University of CINCINNATI
LIBRARY PUBLISHING SERVICES

An imprint of the University of Cincinnati Press

ISSN: 0002-9726

Communications for Journal Publication

Manuscripts, Technical Notes and Trade News Releases should contact:

Mr. Steven D. Lange, Journal Editor, c/o University of Cincinnati, 5997 Center Hill Ave., Bldg. C, Cincinnati, OH 45224, USA
E-mail: jalcaeditor@gmail.com Mobile phone: (814) 414-5689

Contributors should consult the Journal Publication Policy at:
http://www.leatherchemists.org/journal_publication_policy.asp

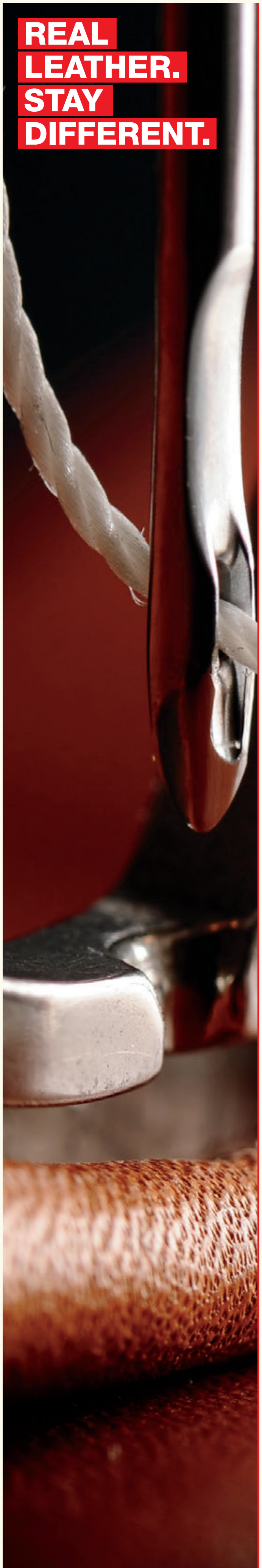

LEATHER BY NUMBERS:

FACTS AND FIGURES FROM THE US LEATHER INDUSTRY AND BEYOND

Note: All figures as of January 2021 or latest available.

ZERO cattle are killed to make US leather. US hides have been valued at JUST 1-2% of a cow's total value for the last two years, which is why they are considered a by-product and often end up as waste. The average price per head of US cattle is $2,000-2.200, while hides vary in price from $5 TO $35 PER PIECE, if sold at all. (1)

330M hides come from the meat and dairy industries around the world. Approximately **34M** were processed the US. (2) **AS MANY AS 2.4M US HIDES** ended up as landfill in 2019, this is **7%** of the national total.

Worldwide the waste figure is approximately **40%** or **132M** hides. With the average hide weighing 25Kg this means that **3M TONNES** are thrown away ever year.

Leather production turns more than **4.5M TONNES OF** potential waste, every year, into usable, durable goods. This saves **2.7M TONS OF GREENHOUSE GAS EMISSIONS** from landfill sites. (3)

Production, processing and distribution of hides and leather products directly employs an estimated **5,486** individuals, who collectively earn more than **$384M**. US exports of hides and leather was over **$1.5BILLION** in 2021. (4)

The US exports approximately **95%** of all cattle hide and wet blue leather products it produces, worth **$2.85BILLION**. (5)

Around **45%** of global leather production is used to make footwear, **22%** for clothing, bags and accessories, **18%** for car upholstery, and about **15%** for furniture. (6)

Water consumption for the production of leather from cattle hides has fallen by more than **35%** in the past 25 years, down from **60 CUBIC-METERS** per ton of hides to **38 CUBIC-METERS** per ton. US tanneries are required, by law, to connect to effluent treatment plants to prevent pollution. (7)

Leather will biodegrade in **LESS THAN 50 YEARS**. In contrast, it can take **500 YEARS** or more for synthetics, made from petrochemicals, to degrade. (8)

ReFed's conversion rate for food waste is for **EACH METRIC TON OF WASTE DISPOSAL** there is **9.8 7MT** of **CO2 EQUIVALENT** emitted. In this case, mostly as methane. (9)

This factsheet is produced by the Leather and Hide Council of America (L&HCA), established to promote the US leather industry which is responsible for a significant proportion of the international trade in hides. The L&HCA works to establish best practice in US leather production and to share this worldwide. Figures quoted refer to the USA unless otherwise stated.

SOURCE:

(1) https://downloads.usda.library.cornell.edu/usda-esmis/files/rx913p88g/w0893q25p/5d86qb66f/lstk0223.pdf

(2) https://downloads.usda.library.cornell.edu/usda-esmis/files/r207tp32d/pg15cj85z/hd76t466z/lsan0422.pdf

(3) 2020 LHCA Infographic

(4) John Dunham & Associates, Economic Impact of the Meat Industry (2016)

(5) https://thesustainabilityalliance.us/wp-content/uploads/2020/04/US-Hide-Skin-and-Leather-Factsheet-0420.pdf

(6) TBC

(7) 2020 LHCA factsheet

(8) https://en.wikipedia.org/wiki/Leather#:~:text=Leather%20biodegrades%20slowly%E2%80%94taking%2025,or%20more%20years%20to%20decompose

(9) https://insights-engine.refed.org/impact-calculator?inputs=%7B%22sector%22%3A%22manufacturing%22%2C%22type%22%3A%22fresh-meat-seafood%22%2C%22unit%22%3A%22tons%22%2C%22alternative%22%3Afalse%2C%22destinations%22%3A%5B%7B%22key%22%3A%22refuse-discards%22%2C%22current%22%3A1%7D%5D%7D

JOURNAL OF THE
AMERICAN LEATHER CHEMISTS ASSOCIATION

Proceedings, Reports, Notices, and News
of the
AMERICAN LEATHER CHEMISTS ASSOCIATION

THE JOURNAL OF THE AMERICAN LEATHER CHEMISTS ASSOCIATION (USPS #019-334) is published monthly by The American Leather Chemists Association, c/o University of Cincinnati, 5997 Center Hill Ave., Bldg. C, Cincinnati, Ohio 45224. Telephone (513) 290-2505. Single copy price: $10.00 members, $20.00 non-member plus shipping and handling. Subscriptions: $185 for hard copy plus postage and handling of $60 for domestic subscribers and $70 for foreign subscribers; $220 for ezine only; and $240 for hard copy and ezine plus postage and handling of $60 for domestic subscribers and $70 for foreign subscribers.

Periodical Postage paid at Cincinnati, Ohio and additional mailing offices. Postmaster send change of addresses to The American Leather Chemists Association, c/o University of Cincinnati, 5997 Center Hill Ave., Bldg. C, Cincinnati, Ohio 45224.

Website: www.leatherchemists.org E-mail: hallks@ucmail.uc.edu

Microencapsulation of Essential Oils for Antimicrobial Foot Bed

by
Jaffrin Benseelia, B.,[1] Chris Felshia, S.,[1] John Sundar, V.[2] and Gnanamani, A.[1]*
[1]*Microbiology Division, CSIR-CLRI*, Adyar, Chennai
[2]*Leather Processing Technology Division, CSIR-CLRI*, Adyar, Chennai

Abstract

The present study emphasizes the microencapsulation of mixture of three essential oils and explores its application in footwear industry. In brief, essential oils of *Thymus zygis*, *Citrus limonium* and *Cinnamomum cassia* microencapsulated as per the standard protocol followed elsewhere. The obtained microcapsules characterized, fused on to the foot bed materials of footwear using hand sprayer and assessed the antimicrobial property after air-drying. The foot bed material chosen for the present study includes leather, textile and polymer. Representative standard Gram -positive and Gram – negative bacterial species, and few of the fungal species isolated from leather samples are the test organisms used in the present study. Results revealed the size of the microcapsules as 25-60 nm. Optical and Scanning electron micrographs suggested the spherical nature of the capsules. Antibacterial and antifungal activity studies on microcapsules as such and foot bed materials before and after the incorporation of microcapsules infers the complete inhibition of microbial growth in microcapsules incorporated foot bed materials. The stability studies on the spray coating of microcapsules on to the foot bed materials reveal more than six months stability. SEM analysis of fungal species before and after exposure to microcapsules suggested the thinning of filaments and the natural mechanism of growth inhibition. In conclusion, coating of microencapsulated essential oils adds antimicrobial property to the foot bed materials.

Introduction

In the history of human existence, footwear has become an essential commodity in our day-to-day life. It serves in protection as well as comfort to the feet while performing various activities like walking, running and all such essential movements of the human to commute. Further, it protects the feet from hot and cold surfaces, dirt, and injuries associated with them. It also provides comfort in the form of a flat and cushioning effect to feet that helps to walk without any impact from external factors. Majority of footwear available for outdoor activities are closely packed and the poor ventilation grounds lack of oxygen to the human skin, creating a favorable environment for the microbial growth, which in turn causes discomfort as well as potential damage to the footwear. Further, the presence of large number of sweat glands in the human foot causes excessive sweating and unpleasant odor during physical activities. The moist environment and humid condition also facilitate microbial growth, which leads to infections. As this has become prime concern with consumers, varieties of foot deodorizing agents, foot care kits, and hygienic socks are developed commercially to overcome the said disadvantages. The recent report suggested that sanitation of shoe and sock might prevent the superficial microbial infections of the feet.[1] In the current Covid 19 pandemic conditions, all of us have the practice of sanitizing the shoe and socks in a regular manner, however, in real life; the feasibility of applying sanitizers may not be a practical one and cannot be considered as an effective protective system.

Figure 1. Representative images on the components of foot-bed materials used for the preparation of a complete foot-bed. The synthetic foot-bed materials composed of a fabric, lining and foam materials and the leather-based foot-bed material composed of a leather material of bovidae origin

*Corresponding author email: gnanamani3@gmail.com or gnanamani@clri.res.in
Manuscript received October 16, 2023, accepted for publication December 6, 2023.

The foot-bed of footwear is a thin layer of material used to cover the insole. Figure 1 illustrates the type of foot-bed materials used for the manufacturing of footwear. It is the layer that is directly in contact with the sole of the wearer's foot and responsible for the microbial growth mediated discomfort. In order to prevent microbial growth, coating /spraying of chemicals such as pentachlorophenate, cycloheximide, zinc oxide, copper oxide, formaldehyde, hydroxyquinoline or exposure to UV radiation are the procedures suggested, however, the reoccurring nature of the microbes is unavoidable.[1] The commercial antifungal foot-bed products are made up of bamboo, alum and charcoal and were reported for the efficacy in inhibiting the growth of microbes.[2] Developing antimicrobial leathers and antimicrobial fabrics as foot-bed materials are challenging and involve high cost.

Even though during processing of animal skin to leather several biocides are employed, but still fungal infections are of great nuisance.[3] Chemical based antimicrobial compounds and coatings with silver nanoparticles on synthetic fabrics are not effective.[4] Conventionally, foot-bed materials made up of polymers are not susceptible to microbial growth but the non-degradable nature and pollution generation upon usage are the major reasons to prevent use of such material for in-sock material. Literatures suggested incorporation of antimicrobials might be a suitable solution for the preparation of antimicrobial foot-bed.

In healthcare, controlled release of drugs is achieved through microencapsulation technique and deployed for targeted drug delivery.[5] In a similar methodology, microencapsulation of antimicrobials and incorporation to leather and fabric may provide the long-lasting antimicrobial property to foot-bed materials. Zarnecki, et al.[6] studied the use of cream-based antifungals and concluded that use of cream is inconvenient and relapses within a shorter period and need alternatives. Yip et al.[7] prepared hygienic socks based on microencapsulated antifungals and reported the significant effect of the socks on controlling the fungal growth and protect the foot efficiently. In terms of compatibility, selection of antimicrobials plays a major role in in-sock preparations. Medicinal herbal plants and the bioactives are established for antimicrobial activity and most of them are recognized as a generally recognized as safe (GRAS) without side effects. Bielak and Cholewinska[8] studied the antimicrobial effect of essential oils in lining leather and suggested the use of essential oil to prevent fungal growth. Lu et al.[9] studied the antimicrobial activity of nano emulsions incorporating citral essential oil.

Thus, the present study emphasizes microencapsulation of essential oils and explored its application in the preparation of antimicrobial foot-beds. Our recent study (unpublished data) on antimicrobial property of the individual essential oils revealed the differences in antibacterial and antifungal properties when tested with clinical strains. Hence, in the present study an attempt was made on the use of mixture of three essential oils. Microcapsules containing oil mixture comprising of essential oil of *Thymus zygis*, *Citrus limonium* and *Cinnamomum cassia* in equal volume ratio 1:1:1 prepared, characterized and then fused on to the textile, polymer and foam materials and tested for the antimicrobial efficacy as per the standard ASTM procedures. The methods followed and the observations made were detailed in the following paragraphs.

Methods

Chemicals

Commercial grade essential oils of *Thymus zygis*, *Citrus limonium* and *Cinnamomum cassia (M/s. Grassee International*, India, >99% purity) as core material, melamine formaldehyde resin (M/s. Stahl India Ltd.) as shell material and polyvinyl alcohol (M/s. Sd Fine Chemicals, India) as a stabilizer, non-ionic surfactant (Tween 80, M/s. Sd Fine Chemicals, India) for emulsification, were procured and used in the present study. Experimental materials leather, synthetic fabric and foam were procured from SPDC Division, CSIR- CLRI. Microbial strains received from IMTECH, Chandigarh, India.

Emulsion preparation and encapsulation

The core (the oil mixture), shell material (melamine-formaldehyde) and the stabilizer (polyvinyl alcohol) were prepared individually and subjected to the preparation of microcapsules as per the procedure summarized by Hwang et al.[10] In brief, the core material was prepared in the form of emulsion using Tween 80 (1 % w/v) as a hydrophilic emulsifier. The oil mixture (1:1:1) and the water was taken at 1:2 ratio respectively and homogenized with emulsifier in an ice bath using ultrasonicator (M/s. Lark, India) for 10 min. at temperature 25°C with a sonication power of 75%. The emulsion thus obtained was microencapsulated under *in situ* condition using 10 % (w/v) of alkaline melamine-formaldehyde (M/s. Stahl India Ltd., 75% purity) resin (pH 8.0) under stirring condition (200 rpm, Magnetic Stirrer) for the period of 8 hours. Melamine-formaldehyde is an indirect food additive and employed as a stabilizer[11,12] hence chosen for the present study. The encapsulated oil mixture was then stabilized using 0.1% polyvinyl alcohol (M_w=1,25,000; M/s. SD Fine chemicals, India) at pH 5.0 for the period of 2 hours at 50°C. The precipitate formed separated by centrifugation (10000 rpm) and washed with ethanol (30% w/v) (to remove the unreacted components) and dried overnight at 40°C. The resultant microcapsules subjected to characterization and then used for the preparation of antimicrobial foot-bed.[13] In brief, microcapsules were dissolved in aqueous ethanol and sprayed on the chosen experimental materials using a mechanical sprayer. Optimization on number of sprays required for sustainable antimicrobial property calculated accordingly for long time efficacy.

Characterization of microcapsules

Surface morphology of the prepared emulsion followed by *in situ* polymerization was obtained from imaging under optical microscope

(Eclipse Ni microscope, bright field). About 10 microliters of the samples in wet condition were diluted with 0.5ml of deionized water and a drop of the diluted sample viewed and imaged. With reference to scanning electron micrograph, the diluted sample placed on the carbon coated stubs in wet condition and air dried and viewed under Phenom 1817 supplied by Thermo Fisher scientific Pvt Ltd., United States. Scanning electron micrographs of microcapsules before ethanol washing were made to confirm the capsule formation. The colloidal solution obtained was placed on the carbon-coated stubs and upon drying subjected to gold coating and viewed under Field Emission Scanning Electron Microscope at 10 keV.

Size distribution of microcapsules

Dynamic Light scattering (DLS) is a non-invasive, well- established technique for measuring the size and size distribution of molecules and particles typically in the submicron region. In the present study, the size of the prepared microcapsules was measured by dynamic light scattering (DLS), using a Malvern Nano ZS system by Malvern Instruments equipped with a He\Ne 633 nm laser (Malvern Zetasizer Nanoseries, Malvern, U.K.) operated at 25°C.

Storage, Temperature and pH stability assessments

The storage stability of the samples was assessed by placing the transparent glass tubes containing 25 ml of the samples at 4°C and 35°C temperature respectively and observed the stability for the scheduled period of 5, 10 and 15 days for the occurrence of any phase changes. Temperature and pH stability of the microcapsules studied at different temperatures (20, 25, 30, 35, 40 °C) and at pH in the range of 4.0 - 8.0. The samples were kept in glass tubes at respective temperatures for a period of 12 hours and observed for stability. Similarly, for pH stability, the respective sample was diluted with respective pH buffers and stored at different temperatures (20, 25, 30, 35, 40°C) for the period of 6 hours and observed for the occurrence of any phase changes.

Selection of microbial species

To assess the antimicrobial property, the following bacterial and fungal species, viz., *Pseudomonas aeruginosa* (MTCC 1688*), Bacillus subtilis* (MTTC 441*);* and five different fungal species: *Aspergillus niger (*MTCC 282); *Penicillium pinophilum (*MTCC 2009); *Chaetomium globosum (*MTCC 155); *Auresobasidium pullulans (*MTCC 153); *Gliocladium virens (*MTCC 2023) were procured from IMTECH, Chandigarh, India. Followed by procurement, the cultures were sub-cultured in the respective growth medium and were then stocked in a glycerol medium at 4°C until use. For bacterial species nutrient broth served as a growth medium and sabouraud dextrose broth for the growth of fungal species. For antibacterial studies, pre-inoculated cultures grown at 37°C for a period of 18 hours were employed. For antifungal studies, mixed spores stored at 4°C were used for lawn preparation.

Antimicrobial activity of plain essential oils and microcapsules

Antimicrobial activity of the essential oils and the microcapsules containing oil mixture were assessed by well diffusion assay (CLSI 2020)[14] using the selected bacterial and fungal strains. In brief, a lawn of the 18 hours grown chosen bacterial cultures were made in the plates pre-loaded with Mueller –Hinton agar and the well of size 6 - 8 mm using a well borer made aseptically. Respective essential oils and the microcapsules were indented to the individual wells and incubated at 37°C for the period of 24 hours for bacterial cultures and for the period of 96 hours for fungal cultures incubated at 25°C. The clear zone around the well was considered and compared with controls, which includes: surface-active agents, antibiotics (Gentamicin (HiMedia, India) and Fluconazole (Merck, India)), and water.

Preparation of microcapsules fused textile, leather and polymeric materials

Two different methods of incorporation of microcapsules were followed for the experimental materials. For leather material, the microcapsules were incorporated by a spray method during the finishing stage of the leather manufacturing process. For other materials, spraying was done directly on the materials. All the experimental materials received three times spray coating and then subjected for testing. Further, a foot-bed product was prepared using microcapsules fused experimental materials and subjected to antimicrobial studies.

Antimicrobial activity of microcapsules fused experimental materials and the prepared foot-bed

Plate assay

The antimicrobial activity of microcapsules fused experimental material was assessed according to ASTM E2149 method.[15] Followed by spray coating the materials were kept at room temperature for 24 hours and after scheduled time intervals, the samples were exposed to antimicrobial studies by placing the specimen on the pre-lawn cultures and incubated at 37°C and observed the zone of inhibition exhibited by the material and compared with the uncoated material.

Direct method

Further, the microcapsules fused experimental materials were stitched as a foot-bed and subjected to antifungal studies as per ASTM standard methods E2149. In brief, the mixed fungal spore suspension was aseptically sprayed (optimized as three times at the intervals of 1 hr) on the surface of a foot-bed and incubated at 25-27°C with the relative humidity in the range of 85-87% for the time duration of 7 days. After the incubation, ratings were given on the observations made as detailed in Table I. Then, the incubation was extended for a period of 14 -21 days. If nil growth was observed even after 21 days, accelerated testing was followed by indenting the spores again to the same material and continue the incubation for a period of 45 days and observed the growth till the completion of the experimental period.

Hemocompatibility Studies

The hemocompatibility of the microcapsules was assessed according to the standard ISO 10 993–4:2017 procedures using the peripheral blood collected from a healthy volunteer.[16] In brief, the microcapsules

Table I
Rating on microbial growth analysis on test samples

Observed growth on specimen	Ratings
None	0
Traces of growth (Less than 10%)	1
Mild growth (10 to 30%)	2
Medium growth (30 to 60%)	3
Heavy growth (60 to 100%)	4

in triplicates were placed in contact with 5 % human red blood cells (RBC) and incubated at 37°C for 1 hour along with positive and negative controls. The absorbance was measured at 415 nm using a multi-plate reader. The percentage of hemolysis was calculated according to the following equation:

$$\% \text{ Hemolysis} = OD_{test} - OD_{negative} / OD_{positive} - OD_{negative} \times 100$$

Where, OD test corresponds to the optical density of test group containing microcapsules, OD negative refers to the saline control and OD positive stands for Triton-X control group.

Results

Figure 2a, depicts the surface morphology of microcapsules (before stabilization) viewed under optical microscope (40×) and Figure 2b shows the scanning electron micrograph of the microcapsules. The microcapsules were pointless structures with defined outer coatings. The size of the microcapsules measured through dynamic light scattering spectroscopy, which displayed the size ranging from 25-65 nm (Figure 2c).

Thermal stability of the microcapsules was studied at five different temperatures, viz, 4, 20, 30, 37, and 40 °C for 24 hours of incubation and the observation on a nil release of emulsified oil suggested the stability of the microcapsules up to 40°C. No higher temperature stability studies were undertaken since, the temperature of the human foot normally varies from 35- 40°C. Stability studies for pH that were carried out for the pH 4, 5, 6, 7 and 8, demonstrated no phase changes and suggested that the prepared microcapsules were stable for the pHs tested. The environmental (pH and temperature) stability of the microcapsules may be due to the stabilizer (melamine formaldehyde) used in the preparation. With reference to storage stability, the samples stored at 4°C were found stable for the period of more than 90 days.

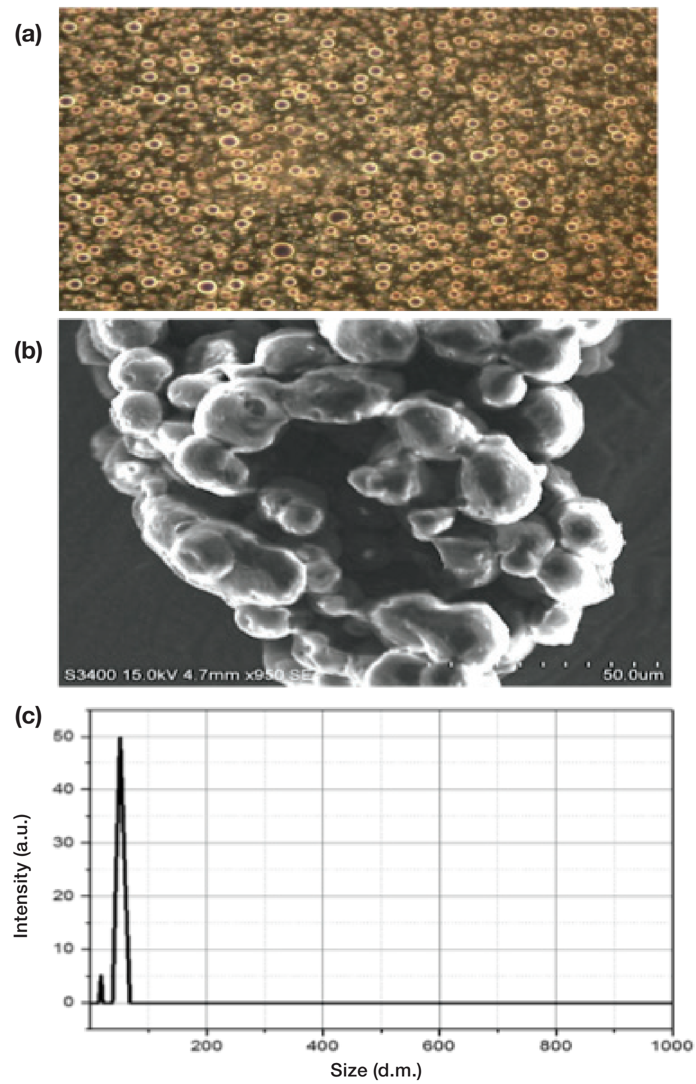

Figure 2. **(a)** Surface morphology of microcapsules prepared using mixed herbal oils and viewed under optical microscope (40× magnifications); **(b)** Scanning electron micrograph of microcapsules prepared and employed in the present study; **(c)** Size distribution of the microcapsules prepared in the present study

Figure 3a & 3b illustrates the preliminary observations on the antimicrobial activity of plain essential oils and the

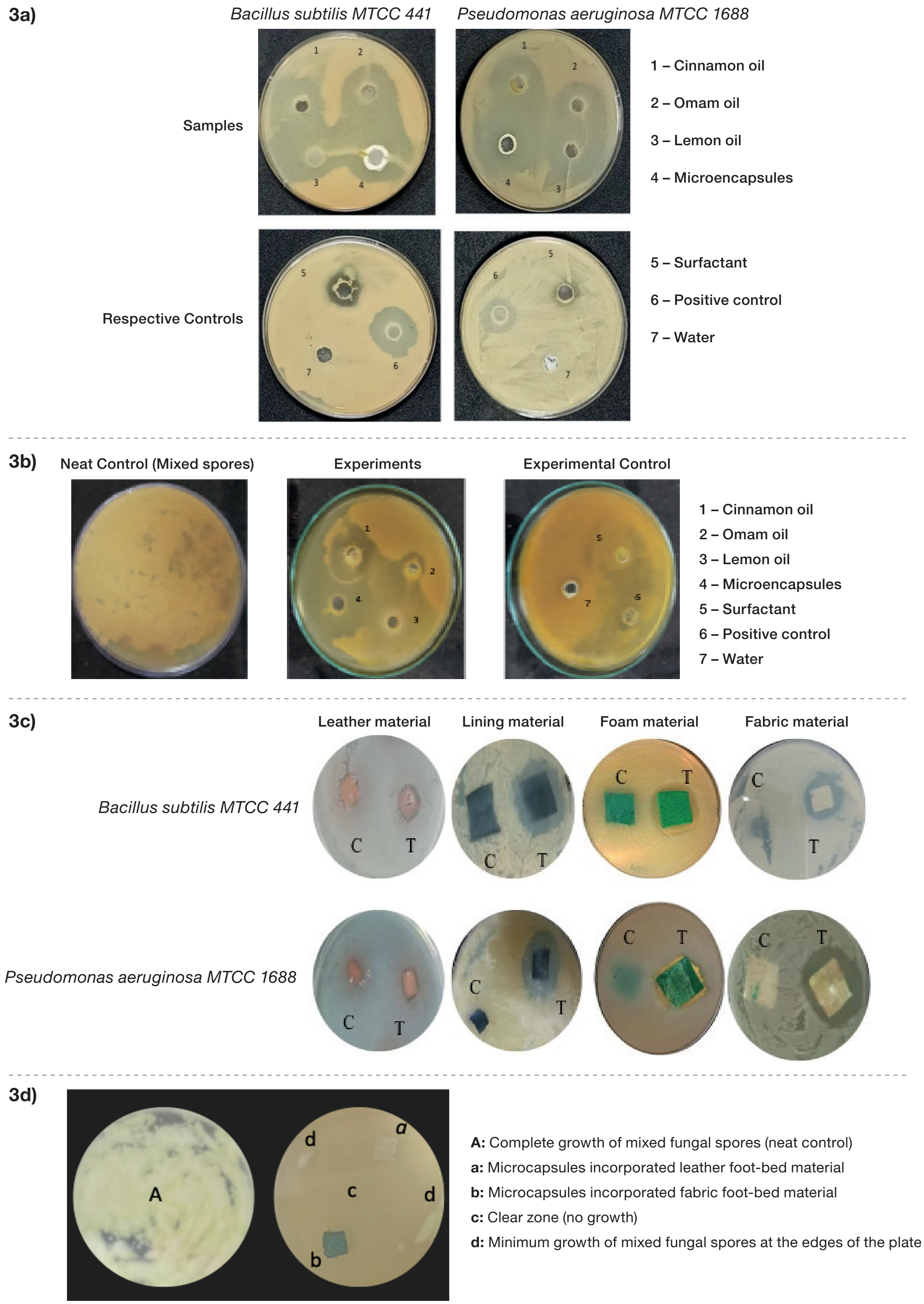

Figure 3. **(3a)** Antibacterial activity (Zone of growth inhibition) of plain individual oil and encapsulated oil mixture (microcapsules) with respect to the chosen bacterial species in comparison with the respective controls; **(3b)** Antifungal activity (Zone of growth inhibition) of microcapsules pertaining to mixed fungal cultures in comparison with the respective controls; **(3c)** Antibacterial activity (Zone of growth inhibition) of the microcaspules incorporated foam, fabric, lining materials and leather (Treated – T) in comparison with the plain material (Contol – C) with respect to the chosen bacterial species; **(3d)** Representative image on the antifungal activity (Zone of growth inhibition) of the microencapsulated (synthetic and leather fot- bed materials) in comparison with the neat control.

microencapsulated oil mixture with respect to bacterial species and the mixed fungal spores chosen for the study. Irrespective the nature of the bacterial species, growth inhibition was exhibited by the individual essential oils as well as with the microencapsulated oil mixtures when compared to a positive control (respective antibiotics) and the surface-active agent used for the preparation of microcapsules. Similarly, the essential oils and the microencapsulated oil mixtures with respect to the mixed fungal spores showed growth inhibition. However, omam oil showed minimum zone of inhibition for mixed fungal spores, however, upon encapsulation as a mixture, a complete inhibition in fungal growth was observed when compared to the respective surface-active agents and the positive control. Figure 3c depicts antibacterial activity of the microcapsules fused foam, fabric, and leather materials in comparison with the plain material and Figure 3d illustrates the antifungal activity in comparison with the control. The microcapsules fused materials display antibacterial and antifungal activities which is similar to the observations made with plain oil and encapsulated oil mixture.

The hemocompatibility of the obtained microcapsules tested using 5% RBCs. The concentration of microcapsules was in the range between 5-15 mg. It has been observed that the cell lysis was below 5% suggesting that microcapsules are compatible with the RBCs at the microcapsule concentration of 15 mg, which indicates the hemocompatible nature of the microcapsules. In the case of positive control (Triton –X) complete lysis was observed.

Figure 4a illustrates the antifungal studies carried out with the product foot-bed prepared using the fused experimental materials stitched as a complete foot-bed. The control samples, i.e., the plain (uncoated) foot-bed material showed growth of fungus, whereas the microcapsules fused materials showed nil growth for 21 days when tested under relative humidity of 85% and moisture content of 75%. Further extending the incubation period did not influence the growth of the applied spores suggesting that the microcapsules fused materials, inhibit the growth of the applied fungal spores. Based on the observations the ratings on the antifungal studies on the prepared product foot-bed materials were given in Table II. The fungal growth in the control samples received 1-3 ratings whereas the ratings of treated samples were observed as zero indicating the efficiency of the microcapsules in preventing and controlling the applied fungal spores. Further, the accelerated testing study carried out suggested that the microcapsules fused foot-bed product exhibited antifungal activity for the experimental period of 45 days.

Figure 5(a-e), illustrates the SEM images observed on different days of the study period of spores applied on the prepared foot-bed product which revealed the impact of microcapsules on the chosen fungal species. Figure 5(a) denotes the control –untreated mixed fungi and 5(b) – 5(e) show the observations made on 7, 14, 21 and 28 days of incubation. The SEM image of control samples display the presence of a complete mixed fungal species with different healthy hyphae structures and spores. However, the fungal spores applied on the microcapsules fused materials (Figure 5b & 5c) showed changes like elongation, initiation of shrinkage after day 7 and day 14 and complete destruction of hyphae structure after day 28 of incubation.

*denotes the growth of the applied mixed fungal spores in the materials free from microcapsules

Figure 4. Antifungal activity of a complete foot-bed materials fused with mixed herbal oil microcapsules in comparison with the materials without microcapsules. The images were taken after day 7 of the experimental period.

Table II

Fungal growth ratings of the experimental samples incorporated with the microcapsules prepared from mixed herbal oils.

Foot-bed Materials	Control	Microcapsules fused materials
Leather	2	0
Synthetic (back side)	3	0
Synthetic (Front side)	1	0

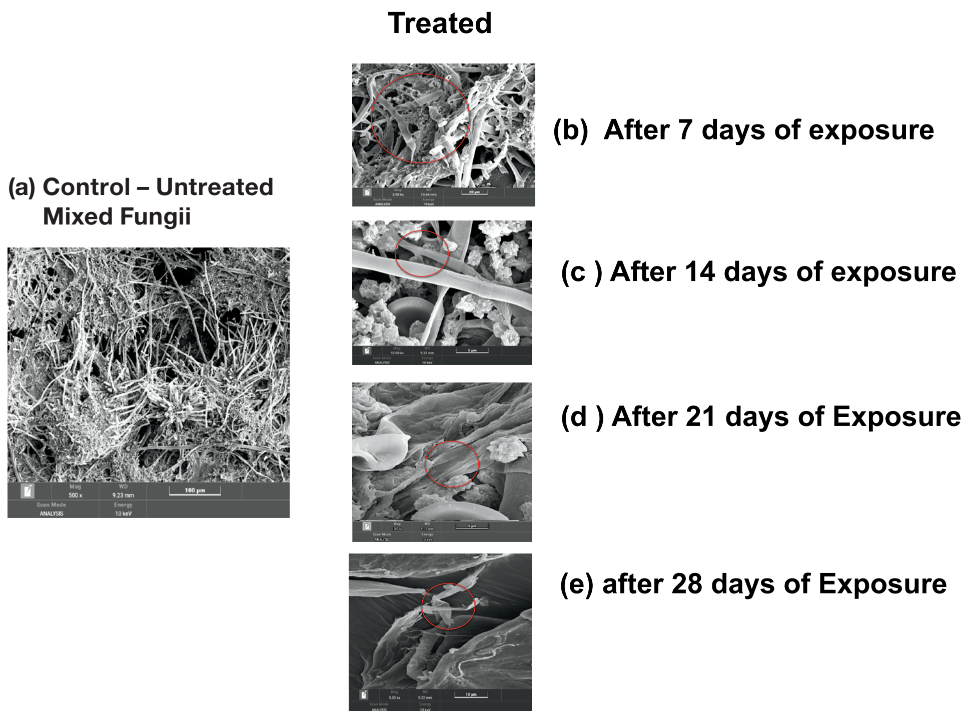

Figure 5. Scanning electron micrograph of fungii species collected from the experimental samples during the course of the study period: **(a)** Control – untreated mixed fungi sample; **(b)** after 7 days; **(c)** after 14 days; **(d)** after 21 days; **(e)** after 28 days; **(f)** Morphology of hyphae in control samples; and **(g)** morphology of hyphae of the samples collected on day 21 of the experimental period of the microcapsules incorporated in-sole samples

Discussion

One of the primary causes for the health-related issue is microbial infections. Hence, attention has been given to control or to prevent microbial infections through numerous approaches. Indenting the antimicrobial property through chemicals or nanoparticles has been accepted, but still intensive research is going on at global level on toxicity of over exposure of antimicrobials on humans. Our recent article explored the various reasons for the development of antimicrobial resistance in Gram-negative pathogens in India.[17]

In recent years, followed by COVID 19 pandemic, natural products gained importance in all aspects of human health care. Natural herbal bio actives though demonstrate microbial growth inhibitions under both *in vitro* and *in vivo* studies, the extended application of use of herbal bio actives in the preparation of antimicrobial materials for the health sector especially in footwear manufacturing process is completely missing. In general, essential oils are effective against microbes. Brut[18] explored the benefits of essential oils as food preservatives and suggested the volatile compounds present in the essential oils are responsible for antimicrobial properties. Citral (an active component of citrus fruit peel oil), damages the lipid bilayer of microbial species and lyses the cells.[19] An attempt on use of natural biocides in footwear showed beneficial effects but the odor and the oily nature are the major drawbacks realized.[8] As a preventive measure, emulsification followed by encapsulation has been suggested. Donsi et al.[20] reported even the low concentrations of essential oil in the form of microcapsules delay the microbial growth or inactivate the microorganisms. Nielsen et al.[21] reported the enhancement of antibacterial efficacy of isoeugenol (bioactives of Cinnamaon oil) upon emulsification and encapsulation. Lu et al.[9] studied the nanoemulsion formulation of Citral essential oil for its antimicrobial activity. Encapsulation of cinnamon essential oil using hydroxypropyl methylcellulose showed enhanced antimicrobial activity.[22]

Based on the described information and the demand for antimicrobial materials, the present study has been taken up to prepare antimicrobial foot-bed material using microencapsulated essential oils. The microcapsules prepared in the present study using mixtures of essential oils of *Thymus zygis*, *Citrus limonium* and *Cinnamomum cassiai* as core material, melamine formaldehyde as the shell material and stabilized with polyvinyl alcohol displayed spherical nature with the capsule size in nanometer. Hu et al.[23] studied the melamine formaldehyde microencapsulated fluorescent dye for its application in cotton fabric printing. Further, a recent report by Sui et al.[24] confirmed the effective role played by melamine formaldehyde in the preparation of microcapsules.

With reference to antimicrobial property, it has been well reported that the nature of phenolic components present in the herbal oils determine the antimicrobial efficacy.[25] Despite the absence of phenolic moieties in omam oil, zone of inhibition shown by omam oil could be due to the presence of phosphorodithioic acid, alkylesters and zinc salts. According to the available literatures, lemon oil has limited antifungal activities, but, Mukarram et al.[26] and Tzortzakis et al.[27] reported growth inhibition of about 47 fungal species by the lemon grass essential oil, but the percentage of inhibition depends on the concentration of the essential oil. However, higher concentration may not be taken for the present study since the odor generation is a major drawback. However, in the present study, all three oils exhibited growth inhibition of both bacteria and fungi and the tests carried out with microcapsules exhibited the antimicrobial property. The appreciable growth inhibition of both bacterial and fungal species shown by cinnamon oil might be due to the presence of volatile compounds, oxygenated compounds, hydrocarbons and cinnamaldehyde. Nabavi et al.[28] reviewed the antibacterial activity of cinnamon and its bioactive including essential oils in detail and revealed the essential oil contain t-cinnamaldehyde, eugenol and few minor compounds like cuminaldehyde and gamma terpinene. Though the reports on cinnamon oil are encouraging, it is advisable to use in minimum doses. According to Nabavi et al.[28] and Haddi et al.[29] ingestion of cinnamon oil may cause depression in the central nervous system. In the present study, the quantity of each oil taken in equal proportions and the encapsulating efficacy calculated as 67±6%. With that percentage, the microcapsules exhibited growth inhibition at significant level. The hemocompatibility studies revealed that there was nil lysis up to 15 mg of microcapsules/ml and assures the compatibility.

From Figure 3c, the zone of inhibition exhibited by the microcapsule fused experimental materials suggests microcapsule incorporation offered antimicrobial properties to the experimental materials. The zone of growth inhibition shown by the mixed fungal spores also support the above statement. Similar observations were made when transforming the experimental material to a complete foot-bed. Microcapsules incorporation did not allow the applied fungal spores to grow and multiply. A complete destruction of fungal hyphae observed after 28 days indicates the effectiveness of microcapsule fused experimental materials in preventing the growth of microorganisms especially the mixed fungal spores. In order to assess impact of applied microcapsules on fungal spores, the fungal spores were collected from Day 0, 7, 14, 21 and 28 of exposure to microcapsule fused experimental material and viewed under scanning electron microscopy. The images displayed a significant change in hyphal structures, which is similar to the observations on change and damage in hyphae morphology in the presence of antifungal agents in the form of essential oil.[30-32] The complete damage in the hyphae structure after 28 days of incubation could be the major reason for the growth inhibition observed with microcapsules incorporated foot-bed materials.

Conclusion

In the present study an attempt was made to explore the use of essential oils for the preparation of antimicrobial materials. The first step involved microencapsulation of a mixture of *Thymus zygis*, *Citrus limonium* and *Cinnamomum cassiai* essential oils. The encapsulated oil was then fused with the experimental materials like textile (fabric), leather and polymeric (foam) by spray coating. The resultant fused material was then subjected to product development in the form of a foot-bed. All the prepared items (plain oil, microencapsulated oil, microcapsules fused textile, leather and polymeric materials and a foot-bed product prepared using the microcapsules fused materials) were subjected to antibacterial and antifungal assessment. The results revealed that microencapsulation of essential oils alleviate the application and the appearance of the materials (free from greasy touch). The microcapsules are highly stable up to pH 8.0 and temperature up to 40°C. Upon fused with experimental materials the materials exhibit antimicrobial activity which is very similar to the plain oil /microencapsulated oil. The foot-bed product developed using the fused material demonstrated antifungal activity when tested with the mixed fungal spores and the SEM examination of fungal spores collected from the material after different periods of incubation revealed the complete destruction of fungal hyphae and lose of hyphal integrity. Further, the antimicrobial property of the product developed was realized up to the period of six months of storage. Thus, encapsulation of essential oils finds application in the preparation of antimicrobial materials which finds application in the preparation of medicated foot-bed.

Acknowledgements

Ms Jaffrin Benseelia acknowledges CSIR-CLRI for the permission granted to carry out her M.Tech footwear course and the project at CSIR-CLRI. All the authors thank Caters Department, CSIR-CLRI and CSIR, New Delhi to carry out the study.

Funding Information

The study has been undertaken using the fund allocated under MLP project of CSIR-CLRI.

Author contributions

Dr. Gnanamani: Idea generation, procurement, methods of standaridization and finalization of the manuscript

Ms. Jaffrin Benseelia: Execution of the study, analysis, draft manuscirpt preparation

Dr. Chris Felshia: Execution of study with respect to antimicorbial evaluation, draft manuscript preparation

Dr. John Sundar: Execution of the study in leather and fabric material

Conflict of Interest

All the authors have no conflict of interest.

Data Availability

All of the experimental data are available with the corresponding author and it can be shared upon request.

References

1. Gupta AK, Versteeg SG. The role of shoe and sock sanitization in the management of superficial fungal infections of the feet. *J Am Podiat Med Assn*. **109**(2):141-9, 2019.
2. https://www.amazon.com/Antifungal-Insoles-Charcoal-Athletes-Kaps/%20dp/B07FKLNGRZ
3. Orlita A. Microbial biodeterioration of leather and its control: a review. *Int Biodeter Biodegr*. **53**(3):157-63, 2004.
4. Lemire JA, Harrison JJ, Turner RJ. Antimicrobial activity of metals: mechanisms, molecular targets and applications. *Nat Rev Microbiol*. **11**(6):371-84, 2013.
5. Singh MN, Hemant KS, Ram M, Shivakumar HG. Microencapsulation: A promising technique for controlled drug delivery. *Res Pharma Sci*. **5**(2):65-77, 2010.
6. Zarnecki G, Peters ER. Footcare for people with profound impairment. In: Profound Retardation and Multiple Impairment, (pp. 246-257). Springer, Boston, MA, 1987.
7. Yip J, Luk MY. Microencapsulation technologies for antimicrobial textiles. In: Sun, G. editor. Antimicrobial textiles Woodhead Publishing, pp. 19-46, 2016.
8. Bielak E, Syguła-Cholewińska J. Antimicrobial effect of lining leather fatliquored with the addition of essential oils. *Biotechnol Food Sci*. **81**(2):149-57, 2017.
9. Lu WC, Huang DW, Wang CC, Yeh CH, Tsai JC, Huang YT, Li PH. Preparation, characterization, and antimicrobial activity of nanoemulsions incorporating citral essential oil. *J Food Drug Anal*. **26**(1):82-9, 2018.
10. Hwang JS, Kim JN, Wee YJ, Yun JS, Jang HG, Kim SH, Ryu HW. Preparation and characterization of melamine-formaldehyde resin microcapsules containing fragrant oil. *Biotechnol Bioprocess Eng* 2, **11**(4):332-6, 2006.
11. Andersen FA. Final report on the safety assessment of melamine/formaldehyde resin. *J Am Coll Toxicol*. **14**(5):373-85, 1995
12. Department of Health and Human Services. Indirect food additives: *Polymers- Federal Register*, **52**:4492-4493, 1987
13. Chirila C, Berechet MD, Deselnicu V. Thyme essential oil as natural leather preservative against fungi. In: International Conference on Advanced Materials and Systems (ICAMS) 2016 (pp. 227-232). The National Research & Development Institute for Textiles and Leather-INCDTP.
14. Clinical and Laboratory Standards Institute. Performance standards for antimicrobial susceptibility testing. CLSI supplement. ISBN 978-1-68440-066-9, 2020.
15. Damian L, Patachia S. Method for testing the antimicrobial character of the materials and their fitting to the scope. *Bull Transilvania Univ Brasov. Eng Sci Series I*. **7**(2):37-44, 2014.
16. Escudero-Castellanos A, Ocampo-García BE, Domínguez-García M, Flores-Estrada J, Flores-Merino MV. Hydrogels based on poly (ethylene glycol) as scaffolds for tissue engineering application: biocompatibility assessment and effect of the sterilization process. *J Mater Sci: Mater Med*. **27**(12):1-10, 2016.
17. Periasamy H, Gnanamani A. Polymyxins resistance among Gram-negative pathogens in India. *The Lancet. Infect Dis* 2020; DOI: 10.1016/s1473-3099(20)30855-0
18. Burt S. Essential oils: their antibacterial properties and potential applications in foods—a review. *Int J Food Microbiol*. **94**(3):223-53, 2004.
19. Saddiq AA, Khayyat SA. Chemical and antimicrobial studies of monoterpene: Citral. Pesticide. *Biochem Physiol*. **98**(1):89-93, 2010.
20. Donsì F, Annunziata M, Vincensi M, Ferrari G. Design of nanoemulsion-based delivery systems of natural antimicrobials: effect of the emulsifier. *J Biotechnol*. **159**(4):342-50, 2012.
21. Nielsen CK, Kjems J, Mygind T, Snabe T, Schwarz K, Serfert Y, Meyer RL. Enhancing the antibacterial efficacy of isoeugenol by emulsion encapsulation. *Int J Food Microbiol*. 229:7-14, 2016.
22. Li S, Zhou J, Wang Y, Teng A, Zhang K, Wu Z, Cheng S, Wang W. Physicochemical and antimicrobial properties of hydroxypropyl methylcellulose-cinnamon essential oil emulsion: effects of micro- and nanodroplets. *Int Food Eng*. **15**(9) Article ID: 20180416, 2019.
23. Hu A, Peng H, Li M, Fu S. Preparation of melamine-formaldehyde encapsulated fluorescent dye dispersion and its application to cotton fabric printing. *Color Technol*. **135**(2):103-10, 2019.
24. Sui C, Preece JA, Zhang Z, Yu SH. Efficient encapsulation of water-soluble inorganic and organic actives in melamine formaldehyde-based microcapsules for control release into an aqueous environment. *Chem Eng Sci*. 229: Article ID 116103, 2021.

25. Chouhan S, Sharma K, Guleria S. Antimicrobial activity of some essential oils—present status and future perspectives. *Medicines*, **4**(3):58, 2017.
26. Mukarram M, Choudhary S, Khan MA, Poltronieri P, Khan MM, Ali J, Kurjak D, Shahid M. Lemongrass essential oil components with antimicrobial and anticancer activities. *Antioxidants* **11**(1):20, 2021.
27. Tzortzakis NG, Economakis CD. Antifungal activity of lemongrass (Cympopogon citratus L.) essential oil against key postharvest pathogens. *Innov Food Sci Emerg Technol.* (2):253-8, 2007.
28. Nabavi SF, Di Lorenzo A, Izadi M, Sobarzo-Sánchez E, Daglia M, Nabavi SM. Antibacterial effects of cinnamon: From farm to food, cosmetic and pharmaceutical industries. *Nutrients*, **7**(9):7729-48, 2015.
29. Haddi K, Faroni LR, Oliveira EE. Cinnamon oil. In: Green pesticides handbook CRC Press 2017 pp. 117-150..
30. Tandon VK, Maurya HK, Tripathi A, ShivaKeshava GB, Shukla PK, Srivastava P, Panda D. 2, 3-Disubstituted-1, 4-naphthoquinones, 12H-benzo [b] phenothiazine-6, 11-diones and related compounds: synthesis and biological evaluation as potential antiproliferative and antifungal agents. *Eur J Med Chem* 2009; **44**(3):1086-92.
31. Soylu S, Yigitbas H, Soylu EM, Kurt Ş. Antifungal effects of essential oils from oregano and fennel on Sclerotinia sclerotiorum. *J Appl Microbiol* 2007;**103**(4):1021-30.
32. Romagnoli C, Bruni R, Andreotti E, Rai MK, Vicentini CB, Mares D. Chemical characterization and antifungal activity of essential oil of capitula from wild Indian Tagetes patula L. *Protoplasma* 2005; **225**(1):57-65.

Decoding Source of Leather Odor: A Quantitative Analysis with Heracles NEO

by

Haonan Shi,[1] Haiming Cheng*[1] and Jin Zhou*[1]

[1]*National Engineering Laboratory for Clean Technology of Leather Manufacture, Sichuan University,*
Chengdu 610065, Sichuan, China

Abstract

Leather products are widely used in our daily life and in close contact with users, but the pleasant feeling during its usage is severely affected by the odor volatilized from the leather surface. In this study, a quantitative analysis method to investigate the differences in the odor profiles among four types of leather was proposed. The primary olfactory constituents of four leather types were examined by Heracles NEO ultra-fast gas-phase electronic nose, including Principal Component Analysis (PCA) and Discriminant Factor Analysis (DFA). In chrome-tanned cattle hide leather, the substance with the highest content was 2,4-Dinitrotoluene, while methyl dodecanoate was the predominant compound in chrome-free cattle hide leather. Notably, chrome-tanned sheepskin leather exhibited higher levels of dodecanal, clopyralid, n-octylbenzene, propyl cinnamate, and 3-methylhexadecane. Similarly, chrome-free sheepskin leather contained higher levels of dodecanal, clopyralid, n-octylbenzene, propyl cinnamate, 3-methylhexadecane, and tetradecanol. These findings indicate that each of the four types of leather possesses distinctive compounds, while also sharing common compounds. Furthermore, the results indicate that radar plots along with PCA and DFA analyses can effectively differentiate between the four types of leather.

1 Introduction

The smell and odor of leather products, such as furniture, handbags and footwear, has been paid a growing concern since consumers are increasingly demanding high-performance products.[1] However, leather has been made by a series of processes such as unhairing, liming, deliming, bating, pickling, chrome tanning, retanning, fatliquoring, dyeing, and finishing, in which a large number of chemicals are added, and impart leather products with unique smell.[2] The odor volatilized from footwear can cause dizziness, nausea and other adverse reactions and make it difficult to gain an advantage in sales.[3]

Throughout the leather production process, a multitude of chemicals are both generated and introduced. For instance, in the unhairing process, inorganic sulfides are employed as hair-burning agents, and may produce hydrogen sulfide during the process.[4] Moreover, this process also leads to the formation of ammonia gas due to the reaction between proteins and alkalis.[5]

During chrome-tanning process, acidic odor in leather primarily originates from acidic substances in the tanning agents.[6] Formaldehyde-containing chemicals are also introduced during retanning, neutralization, and dyeing processes.[7]

In processes like fatliquoring, dyeing and finishing, distinct agents are incorporated into the leather. Fatliquoring involves the application of animal and plant fats and oils, resulting in the production of fatty odors.[8,9] The dyeing process employs aldehyde and benzene compounds as pigments, giving rise to the creation of organic compounds like toluene, xylene, and formaldehyde.[10] These substances might linger on the leather surface, decomposing or oxidizing under high temperatures or light exposure, producing odorous compounds such as phenol and pyridine.[11] In the softening phase, waxes and oils are added, leading to the emission of a waxy odor from the leather.[12]

Current assessment predominantly hinges upon subjective appraisals conducted by evaluators' olfactory senses, which is aimed at discerning favorable from unfavorable aromas.[13] However, the reliability of those outcomes is poor; moreover, this method might be unhealthy to the assessors and only a limited array of odorant substances can be identified. As a result, the task of objectively quantifying the attributes of olfactory emanations arising from leather-based articles remains a formidable challenge. Therefore, it is necessary to propose an objective quantitative analysis to evaluate the odor of leather and leather products.[14]

Electronic nose technology transforms subjective odor analysis into quantitative and qualitative data.[15] It has been widely adopted in the fields of food and medicine, enabling rapid and objective assessment of

*Corresponding authors email: chenghaiming@scu.edu.cn (H. Cheng) & zj_scu@qq.com (J. Zhou)
Manuscript received September 13, 2023, accepted for publication December 10, 2023.

product quality.[16-18] The Heracles NEO is an efficient tool that combines GC-MS and electronic nose capabilities, allowing for the swift separation and identification of components within volatile substances.[19] By collecting Kovats retention indices and qualitatively examining chromatographic peaks through the AroChemBase database, this method can derive corresponding substance compositions and odor information. Compared to traditional chromatographic methods, Heracles NEO offers advantages such as minimal sample usage, shorter detection times, simplified preprocessing, and the absence of additional reagent consumption. Therefore, Heracles NEO presents a feasible approach for identifying leather odors.

Given the limited existing research on leather odors, the purpose of this study was to investigate the variations in odor profiles among four types of leather with chrome-tanned or chrome-free leathers, and then to identify the primary odor volatile components.

2 Experimental

2.1 Materials and sampling process

Chrome-tanned cattle hide leather (CTCL), chrome-tanned sheep leather (CTSL), chrome-free cattle hide leather (CFCL), and chrome-free sheep leather (CFSL) were purchased from the local market. In addition, 20 mL headspace vials and screw caps equipped with silicone/Teflon septa (Palo Alto, CA, USA), n-alkane mixture (C6-C16) (A10142930, Restek, USA), equipped with a sealed bag were prepared.

Leather samples were cut into small pieces of approximately 0.5 × 0.5 cm in size. Then, 0.6 g of leather samples were put into a 20 mL headspace vial for the electronic nose, approximately one third of the total volume of the feed vial, sealed via a PTFE spacer, and the prepared sample was placed on the autosampler unit to be analyzed.

2.2 Heracles NEO instrumentation and settings

In this study, the odor analysis was conducted using a Heracles NEO electronic nose (Alpha M.O.S., France). The instrument was equipped with an automated sampling unit, an ultrafast GC system, as well as two flame ionization detectors (FIDs) and two distinct polar columns (MXT-5 and MXT-1701). The integration of classical GC functions and advanced data processing software within the instrument enabled a comprehensive analysis of the collected data.

The experiments were conducted based on pre-established parameters (Table I) that were optimized for the assessment of leather odor.

Table I
The set parameters of Heracles NEO

Parameters	Numerical values
Headspace generation	
Injection bottle volume	20 mL
Sample size	0.6 g
Heating and oscillation temperature	80°C
Heating and oscillation time	20 min
Feeding samples	
Injection volume	5000 μL
Injection speed	500 μL/s
Inlet temperature	200°C
Feed duration	15 s
Trap	
Initial temperature	40°C
Diversion	10 mL/min
Catch duration	20 s
Final temperature	240°C
Column temperature	
Initial temperature	40°C (5 s)
Procedure heating up	1.0°C/s -80°C (0 s)
	2.0°C/s -250°C (30 s)
Collection time	160 s
Detectors	
Detector temperature	280°C
FID gain	12

2.3 Data Analysis and Comparison

The Heracles Neo ultra-fast GC e-nose compensates for the inability of sensor-based e-noses to qualify by quickly obtaining GC information on the target, calibrating it with n-alkane standard solutions (nC_6 to nC_{16}), converting retention times to Kovats retention indices, and generating qualitative results from the AroChemBase database.[19] The AroChemBase database is a Kovats RI qualitative library of millions of constituent odor profiles of compounds assessed by professional odor tasters. The AroChemBase database is a qualitative database of Kovats RI. For data analysis, a method of data radar plots, PCA and DFA, was applied.

Chemical pattern recognition uses data radar plots to visualize the odor composition based on available data. Combining the efficient separation capabilities of gas chromatography with the biomimicry of odors, the Heracles NEO electronic nose provides a comprehensive odor profile of volatile compounds. PCA is a commonly used data dimensionality reduction method and data pre-processing technique that converts high-dimensional data into low-dimensional data while retaining the primary information of the original data. DFA is a method of multivariate statistical analysis, which is based on multivariate analysis, where a set of discriminant factors are identified to discriminate between different groups of samples.[20]

3 Results

3.1 Qualitative analysis of volatile compounds by Heracles NEO e-nose

A comparison of the retention parameter profiles of MXT-5-FID1 and MXT-1701-FID2 in Figure 1 and Figure 2 showed that there was a large difference in odor between cattle hide leathers and sheep leathers, while there were similar profiles between CTCL and CFCL, and between CTSL and CFSL. The content of the odor components

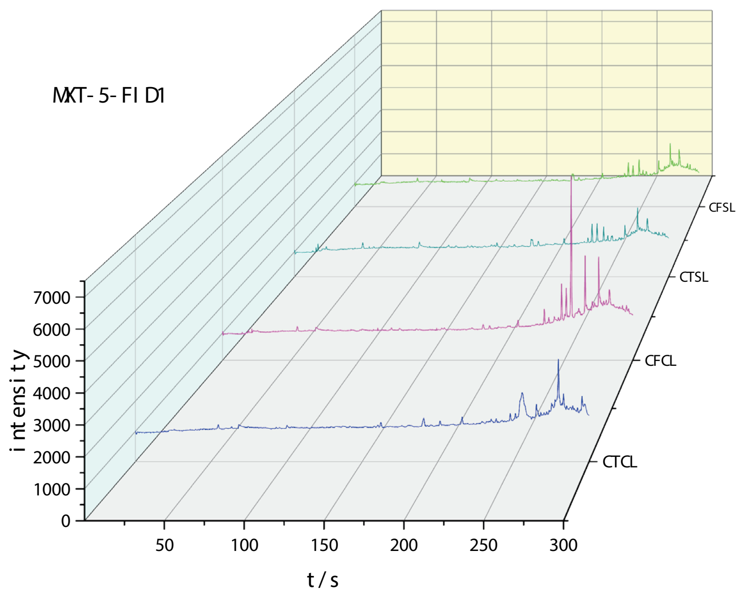

Figure 1. The odor fingerprint of CTCL, CFCL, CTSL and CFSL obtained by the MXT-5

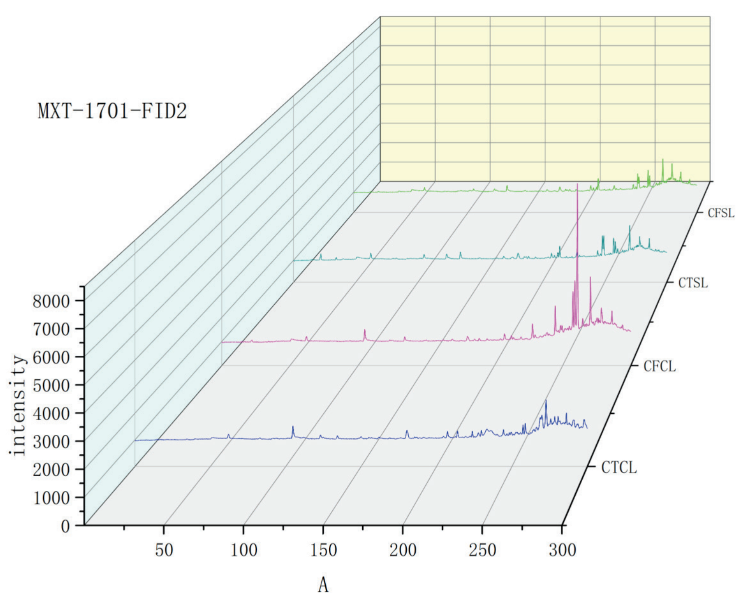

Figure 2. The odor fingerprint of CTCL, CFCL, CTSL and CFSL obtained by the MXT-1701

could be inferred from the peak values of the peaks, the higher the content of the odor components the greater the chromatographic stimulus and the higher the peak.

Table II and Table III described the peak location of CTCL and CFCL and the corresponding possible compounds and their relative contents. In this context, it is notable that both CTCL and CFCL shared the same peak values in the MXT-5 analysis, specifically at 767, 1198, 1298, 1475, and 1497. Similarly, in the MXT-1701 analysis, the shared peak values were 822, 1298, and 1677. These data indicated the presence of identical odoriferous components in the two types of leather. The preliminary analysis suggested that the shared substances included 2-Decanol, Pentadecane-3-Tetradecanol and Toluene.

Based on the data from Tables II and III, it was evident that the potential primary constituents of the odor emitted from CFCL included (E,E)-2,4-Hexadienal, Fenugreek lactone, L-Carvone, (E,Z)-2,4-decadien-1-al, Methyl laurate, 2,4-Dinitrotoluene, Heptyl octanoate, Butyl cinnamate, Methyl tetradecanoate, n-octadecane, and 3-Methyltetradecane. Significantly, 2,4-Dinitrotoluene exhibited a higher concentration, accounting for 47.3% in MXT-5 and 27.59% in MXT-1701. This substance was characterized by an unpleasant and pungent odor.

In contrast, the main odor constituents in CFCL included (*E,E*)-2,4-Nonadienal, delta-octalactone, Skatole, Propyl nonanoate, Propyl decanoate, beta-Himachalene, Methyl dodecanoate, Hexadecane, tetrachloro-m-xylene, and 6-methyl hexadecane. Among these, Pentadecane, Methyl dodecanoate, Hexadecane, and 3-Methylhexadecane were present in relatively higher proportions. Specifically, Methyl dodecanoate had the highest

Table II

Possible volatile compounds identified in CTCL and relative contents

No.	MXT-5		MXT-1701		Possible compounds	Sensory descriptions	Relative content (%)	
	RT	RI	RT	RI			MXT-5	MXT-1701
1	54.84	767	62.07	822	Toluene	Paint; Rubber; Solvent; Sweet	2.51	4.42
2	100.3	915	134.23	1049	(*E,E*)-2,4-Hexadienal	Orange; flowering, vegetative; spicy; sweet	2.32	2.97
3	162.38	1105	213.93	1329	Fenugreek lactone	burnt; caramel; caramel; coffee; marshmallow; maple	3.26	5.69
4	190.68	1198	207.23	1298	2-Decanol	Alkanes; Miscellaneous alcohols	7.21	6.59
5	201.36	1240	223.77	1377	L-Carvone	Herbaceous; Liquorice; minty	2.95	4.40
6	216.12	1298	233.39	1429	(*E,Z*)-2,4-decadien-1-al	Greasy; metal; candle	5.20	7.00
7	247.88	1475	244.37	1495	Pentadecane	Alkanes; Miscellaneous alcohols	3.91	5.05
8	257.54	1541	258.77	1595	Methyl laurate	Soap; sweet; candle scented.	3.16	7.83
9	255.76	1528	272.61	1692	2,4-Dinitrotoluene	Unpleasant smell	47.30	27.59
10	275.18	1670	281.89	1758	Heptyl octanoate	Fresh; freshly cut green grass; greasy	2.29	3.13
11	275.76	1674	293.75	1841	Butyl cinnamate	Fruit; Spicy	2.79	3.76
12	277.58	1688	286.09	1787	Methyl tetradecanoate	Brandy wine; floral, botanical	4.64	6.22
13	283.16	1729	290.67	1819	*n*-octadecane	Alkanes; Fruits; Fuel oil flavor; Miscellaneous alcohols	6.30	5.83
14	251.41	1497	244.52	1496	3-Methyltetradecane	Alkanes; Miscellaneous alcohols	3.16	5.05
15	265.18	1597	275.71	1714	3-Tetradecanol	Fresh; Sweet	3.01	4.48

relative content, constituting 38.47% in MXT-5 and 38.55% in MXT-1701. Interestingly, this compound imparted a relatively pleasant fragrance characterized by notes of wine and floral scents.

Table IV and Table V delineated the peak values and the corresponding potential substances along with their relative abundances in CTSL and CFSL. Specifically, within the MXT-5 analysis, the shared peak values were 768, 915, 1216, 1299, 1417, 1443, 1475, 1596, and 1669. In the context of the MXT-1701 analysis, the corresponding shared peak values were 822, 958, 1529, 1585, 1676, and 1732. Preliminary analysis indicated the presence of common substances, including Toluene, 3,3-Diethylpentane, Methyl nonanoate, Cinnamaldehyde, Dodecanal, Clopyralid, *n*-Octylbenzene, Propyl cinnamate, and 3-Methylhexadecane.

Distinctly, only CTSL exhibited the odoriferous substances Acetone, 2-Dodecanone, and 2-Tridecanone. The odoriferous constituents with the highest content in CTSL encompassed Dodecanal, Clopyralid, n-Octylbenzene, Propyl cinnamate, and 3-Methylhexadecane. Their aromas primarily constituted a blend of aromatic hydrocarbons reminiscent of paints and spices. Conversely, solely CFSL contained the odoriferous substances Skatole, Propyl cinnamate, delta-Undecalactone, and Tetradecanol. Among these, Dodecanal, Clopyralid, n-Octylbenzene, Propyl cinnamate, 3-Methylhexadecane, and Tetradecanol exhibited elevated concentrations. The aromas of these substances ranged from petroleum- and pigment-like scents to hydrocarbon-like notes, fatty odors, and some mildly stimulating fragrances.

Table III

Possible volatile compounds identified in CFCL and relative contents

No.	MXT-5		MXT-1701		Possible compounds	Sensory descriptions	Relative content (%)	
	RT	RI	RT	RI			MXT-5	MXT-1701
1	54.84	767	62.07	822	Toluene	Paint; Pungent; Rubber; Solvent; Sweet	1.84	1.96
2	190.68	1198	207.23	1298	2-Decanol	Flower; fruit; alcohols	2.13	2.27
3	195.33	1216	212.38	1321	(*E, E*)-2,4-Nonadienal	Cucumber;greasy; deep-fried; freshly cut grass	1.45	1.33
4	216.13	1298	248.44	1522	delta-octalactone	Dairy products; Greasy; Peach; Sweet	1.96	2.05
5	235.41	1398	264.74	1637	Skatole	Animals; Medicinal; Mothballs; Intense; warm	3.97	3.62
6	238.69	1418	238.64	1460	Propyl nonanoate	Fermented or brewed; muskmelon	1.58	1.42
7	247.88	1475	244.37	1495	Pentadecane	Alkanes; Miscellaneous alcohols	9.47	6.97
8	250.35	1490	254.94	1568	Propyl decanoate	Fruit, sweet	1.39	1.19
9	251.41	1497	257.52	1586	beta-Himachalene	Pine; trees	7.67	9.59
10	255.05	1523	260.8	1609	Methyl dodecanoate	Coconut;Creamy; Greasy; Floral or botanical; Fruits	38.47	38.55
11	265.23	1598	257.52	1596	Hexadecane	None	12.42	12.44
12	266.11	1604	275.2	1711	3-Tetradecanol	Alkane; Fruits	2.19	2.76
13	270.51	1636	278.84	1736	tetrachloro-m-xylene	Aromatics; pungent	2.68	2.22
14	272.07	1648	266.54	1650	6-methyl hexadecane	None	1.87	1.22
15	275.19	1670	270.38	1677	3-Methylhexadecane	None	10.91	12.41

Table IV

Possible volatile compounds identified in CTSL and relative contents

No.	MXT-5		MXT-1701		Possible compounds	Sensory descriptions	Relative content (%)	
	RT	RI	RT	RI			MXT-5	MXT-1701
1	18.95	505	22.05	602	Acetone	Acetone; Ethanol	4.43	5.35
2	54.89	768	62.03	822	Toluene	Paint; Pungent; Rubber; Solvent	5.67	4.62
3	100.29	915	104.99	958	3,3-Diethylpentane	None	4.27	3.36
4	195.53	1216	207.33	1298	Methyl nonanoate	Sweet; tropical; candle-scented	5.84	4.05
5	216.21	1299	244.45	1495	Cinnamaldehyde	Cinnamon; Clove; Spicy	5.09	4.78
6	235.29	1397	244.45	1495	2-Dodecanone	Oranges; Floral or botanical; Fruits	3.95	4.08
7	238.57	1417	248.29	1521	Dodecanal	Aldehyde group; Octanoic acid; Orange; Oily	14.84	16.81
8	242.65	1443	257.33	1585	Clopyralid	Aromatic;aromatic	14.39	13.36
9	247.91	1475	249.44	1529	*n*-Octylbenzene	Amber; Orange; Pepper	10.66	9.95
10	251.25	1496	260.57	1608	2-Tridecanone	Coconut; Dairy; Earthy; Oily	3.43	4.08
11	264.97	1596	278.27	1732	Propyl cinnamate	Peach	9.64	8.81
12	275.05	1669	270.23	1676	3-Methylhexadecane	None	17.78	20.75

Table V

Possible volatile compounds identified in CFSL and relative contents

No.	MXT-5		MXT-1701		Possible compounds	Sensory descriptions	Relative content (%)	
	RT	RI	RT	RI			MXT-5	MXT-1701
1	54.6	766	62.03	822	Toluene	Paint; Pungent; Rubber; Solvent	4.14	4.00
2	100.3	915	104.98	958	3,3-Diethylpentane	butter	3.08	2.55
3	195.48	1216	207.24	1297	Methyl nonanoate	Sweet; tropical; candle-scented	3.71	5.57
4	216.04	1298	244.52	1496	Cinnamaldehyde	Cinnamon; Clove; Spicy	5.36	3.88
5	235.3	1398	264.54	1636	Skatole	Animals; Fecal; Medicinal; Mothballs	2.99	2.71
6	238.52	1417	248.36	1522	Dodecanal	Aldehyde group; Octanoic acid; Orange; Oily	12.34	13.34
7	242.62	1442	257.37	1585	Clopyralid	Aromatic, aromatic	9.88	13.30
8	247.91	1475	249.44	1529	*n*-Octylbenzene	Amber; Orange; Pepper	13.72	10.85
9	265.08	1596	278.32	1732	Propyl cinnamate	Peach	10.64	13.34
10	275.05	1669	270.23	1676	3-Methylhexadecane	None	23.14	20.24
11	265.82	1602	293.68	1841	delta-Undecalactone	Coconut; Creamy; Greasy; Fruits	4.31	3.78
12	276.98	1684	286	1786	Tetradecanol	Coconut; oily fat	6.69	6.46

3.2 Chemical pattern recognition analysis

Figure 3 illustrates the comprehensive radar plots generated from MXT-5 and MXT-1701 analyses of the four leather types, enabling a visual comparison of the distinctions among them. Notably, the odor intensity of CFCL is the highest, with a peak reaching up to 4000 units. In contrast, the odor intensity of chrome-tanned sheep leather and chrome-free sheep leather is comparatively lower. Furthermore, it is evident that discernible differences existed in the volatile components among the four leather types.

3.3 PCA principal component analysis

Figure 4 presents the PCA analysis of the four leather types, yielding a recognition pattern index of 90. The combined contribution of principal component 1 and principal component 3 is 84.444%, indicating a high level of information. The positions of the four leather types are predominantly located in different intervals, signifying that each type of leather possesses unique components allowing for the distinction among them.

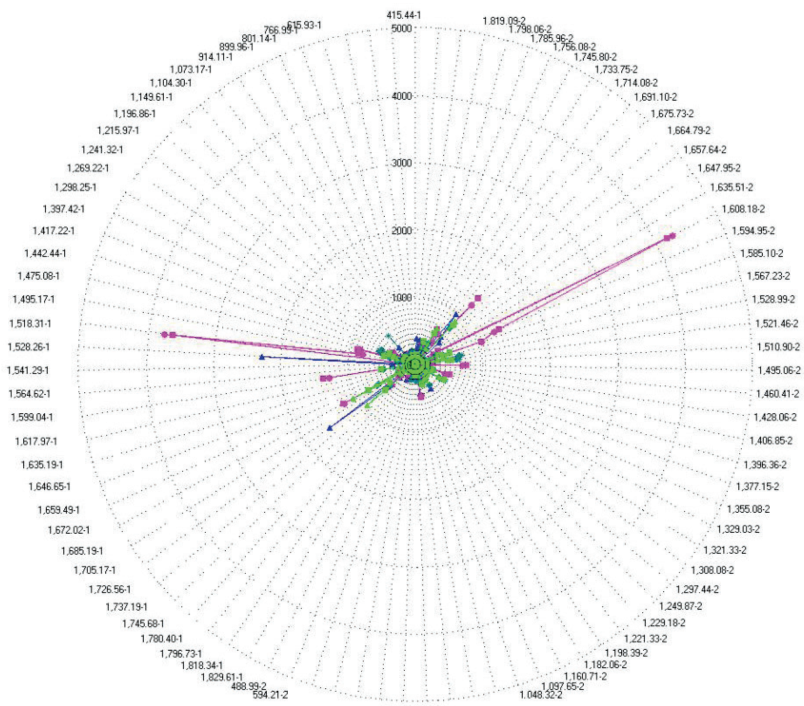

Figure 3. Radar fingerprint map of leather material

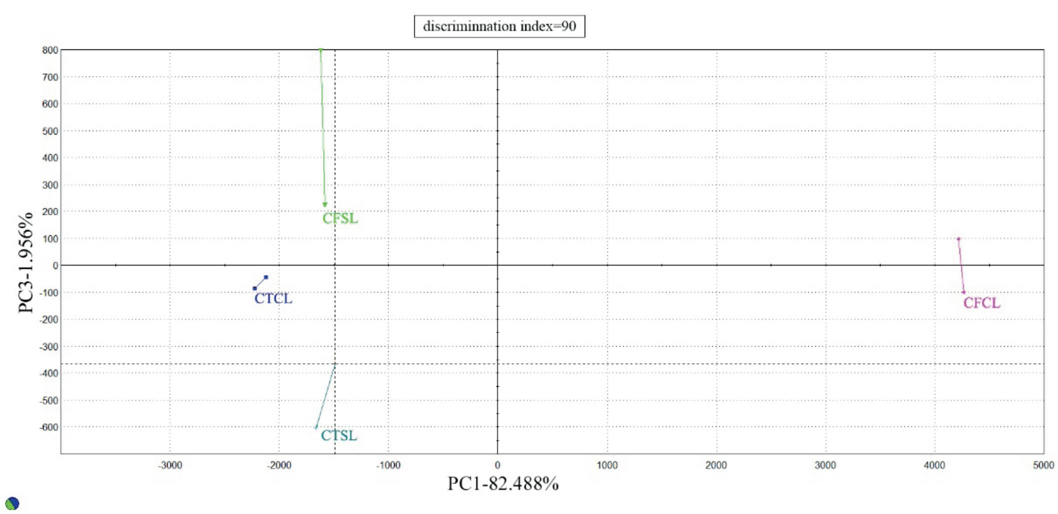

Figure 4. Principal Component Analysis (PCA)

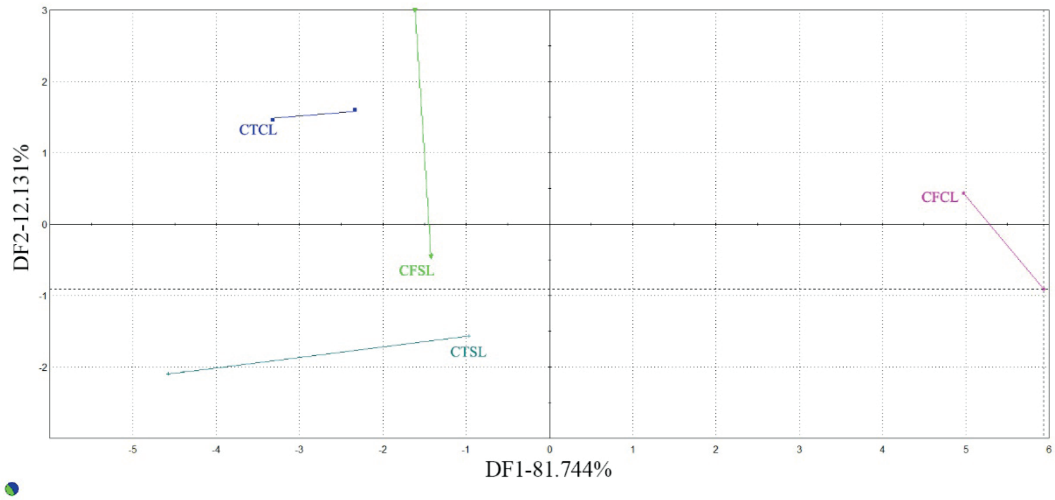

Figure 5. Discriminant analysis (DFA)

3.4 DFA discriminant factor analysis

In the DFA analysis shown in Figure 5, the contributions of discriminant factor 1 and discriminant factor 2 were 93.875%, demonstrating high discriminatory power and indicating clear differentiation among the four leather types.

4 Discussion

Leather is characterized by its numerous volatile components and unique odor. However, current odor evaluation studies in the realm of leather remain largely subjective, relying on experiential assessments, lacking objective quantitative methods. As an emerging technology, Heracles NEO offers advantages such as simple sample preprocessing, convenient instrument operation, rapid detection, and minimal environmental impact. It provides comprehensive odor information about the tested samples and has been applied in fields such as Traditional Chinese Medicine odor analysis, rapid identification, and quality control.

It has been ascertained that benzene-based dyes are employed during the dyeing stage of leather production.[21] In the present study, Benzene-derived volatiles were detected in all leather samples, leading to the preliminary inference that the presence of benzene constituents in leather emissions can be attributed to the dyeing process. Among these, CTCL exhibited the highest concentration of 2,4-Dinitrotoluene at 47.3% for MXT-5 and 27.59% for MXT-1701. Aliphatic hydrocarbons and alcohol volatiles, commonly utilized in leather dyeing and fatliquoring, were also identified in all four leather types.[22] All tested leather samples emitted ester compounds, with a diverse range of types and concentrations. Literature investigation revealed that plasticizers and emulsifiers are commonly employed in leather processing, primarily comprising various organic esters.[23] Among these, Methyl dodecanoate exhibited the highest concentration in chromed bovine leather, at 38.47% for MXT-5 and 38.55% for MXT-1701. CFTL emitted fewer aldehyde compounds, whereas CTCL exhibited a slightly higher presence of aldehyde compounds. Aldehydes are widely utilized as auxiliary tanning agents in leather tanning processes.[7] And CFCL did not use aldehyde tanning agents and related heavy metal salts.

Based on the detected organic compounds, it is hypothesized that these chemicals are a result of the substances used in the tanning and fatliquoring dyeing processes. Due to the similarity in chemical constituents used during processing, different leathers may contain similar volatile components. These substances are highly likely to have formed after the completion of the leather tanning process.

PCA reduces the original data, i.e. the linear combinations that explain the maximum variance of the high-dimensional data to a lower dimension by finding the principal components of the original data, i.e. the linear combinations that explain the maximum variance of the original data, and data down to lower dimensions, thereby reducing redundant information in the data and improving the operational efficiency of the model.[24] DFA is often used for classification or discriminant analysis, for example to classify patients into disease and non-disease groups, or to classify products into different quality levels, etc. DFA can also be used for downscaling and variable selection to help researchers identify the most important variables for discriminating between groups.[25]

It was evident that these odoriferous substances were mostly composed of benzene-derived compounds, alkanes, alcohols, and esters, contributing to the overall leather odor through their mixture. The distinct prominence of different odor constituents among the four leather types indicated substantial differences in odor profiles among different leather types.

5 Conclusion

The quantitative analysis method by Heracles NEO was capable of distinguishing different types of leather produced through different tanning methods. Heracles NEO's electronic nose testing differed from traditional leather odor detection methods; it employed a mechanized and standardized approach, providing objective and visualized results.

References

1. Maraz K. M.; Benefits and problems of chrome tanning in leather processing: Approach a greener technology in leather industry. *Materials Engineering Research* **3**, 156-164, 2021.
2. Hu X., Liu M., Cheng Y., et al.; Light-responsive mesoporous silica nanoparticles loaded with osmanthus fragrance for improving leather odor. *ACS Applied Nano Materials* **5**, 1317-1326, 2022.
3. Domènech R. M. C., Solà A., Otero L. O., et al.; Reducing the use of volatile organic compounds in the leather industry. *Journal of the Society of Leather Technologists and Chemists* **100**, 1–7, 2016.
4. Vijayaraghavan R., Vedaraman N., Muralidharan C., et al.; Aqueous ionic liquid solutions as alternatives for sulphide-free leather processing. *Green Chemistry* **17**, 1001–1007, 2015.
5. Nazer D. W., Al-Sa'ed R., Siebel M. A., et al.; Reducing the environmental and economic impact of the unhairing-liming process in the leather tanning industry. *Journal of Cleaner Production* **14**, 65-74, 2006.
6. Zhang C., Jiang L., Jia X., et al.; A salt-free and chromium discharge minimizing tanning technology: the novel cleaner integrated chrome tanning process. *Journal of Cleaner Production* **112**, 1055–1063, 2016.
7. Sun X., Jin Y., Lai S., et al.; Desirable retanning system for aldehyde-tanned leather to reduce the formaldehyde content and improve the physical-mechanical properties. *Journal of Cleaner Production* **175**, 199–206, 2018.
8. dos Santos L. M., Santos L. M., & Gutterres M..; Reusing of a hide waste for leather fatliquoring. *Journal of Cleaner Production* **15**, 12–16, 2007.
9. Cuq M. H., Benjelloun-Mlayah B., & Delmas M..; Oil extracted from seal hides: characterization and use as leather fat liquor. *Journal of the American Oil Chemists'Society* **75**, 1015–1019, 1998.
10. Chen X., Ding K., & Liu. J.; Synthesis, identification and application of aldehyde reactive dyes. *Dyes and Pigments* **123**, 404–412, 2015.
11. Francesca S., Iacopo C., Alessio C., et al.; Pyrolysis gas chromatography mass spectrometry: A promising tool for disclosing metal-free tanning agents used in leather industry. *Journal of Analytical and Applied Pyrolysis Pyrolysis* **169**, 105803–105803, 2022.
12. Hu Y., Liu J., Li X., et al.; Assessment of the pyrolysis kinetics and mechanism of vegetable-tanned leathers. *Journal of Analytical and Applied Pyrolysis* **164**, 105502–105502, 2022.
13. Verriele M., Plaisance H., Vandenbilcke V., et al.; Odor evaluation and discrimination of car cabin and its components: Application of the ''field of odors''approach in a sensory descriptive analysis. *Journal of sensory studies* **27**, 102–110, 2012.
14. Schropfer M., Czerny M., Schulz H., et al.; The odor of leather. *JALCA* **108**, 94–107, 2013.
15. Karakaya D., Ulucan O., & Turkan M..; Electronic nose and its applications: A survey. *International journal of Automation and Computing* **17**, 179–209, 2020.
16. Sung J., Kim B.-K. et al.; Mass spectrometry-based electric nose system for assessing rice quality during storage at different temperatures. *Journal of Stored Products Research* **59**, 204–208, 2014.
17. John A. T., Murugappan K., Nisbet D. R., et al.; An outlook of recent advances in chemiresistive sensor-based electronic nose systems for food quality and environmental monitoring. *Sensors* **21**, 2271, 2021.
18. Lu L., Hu Z., Hu X., et al.; Electronic tongue and electronic nose for food quality and safety. *Food Research International* **162**, 112214–112214, 2022.
19. Zhang K., Wang J., Fan X., et al.; Discrimination between raw and ginger juice processed Magnoliae officinalis cortex based on HPLC and Heracles NEO ultra-fast gas phase electronic nose. *Phytochemical Analysis* **33**, 722-734, 2022.
20. Slaj M., Spalj S., & Jelusic D..; Discriminant factor analysis of dental arch dimensions with 3-dimensional virtual models. *American journal of orthodontics and dentofacial orthopedics* **140**, 680–687, 2011.
21. Khan S. A., Shahid S., Kanwal S., et al.; Synthesis characterization and antibacterial activity of Cr (III), Co (III), Fe (II), Cu (II), Ni (III) complexes of 4-(2-(((2-hydroxy-5-nitrophenyl) diazenyl) (phenyl) methylene) hydrazinyl) benzene sulfonic acid based formazan dyes and their applications on leather. *Dyes Pigments* **148**, 31–43, 2018.
22. Ke Y., Zhu F., Jiang R., et al.; Determination of polycyclic aromatic hydrocarbons in leather products using solid-phase microextraction coupled with gas chromatography–mass spectrometry. *Microchemical Journal* **112**, 159–163, 2014.
23. Zhang Y., & Wang L..; Recent research progress on leather fatliquoring agents. *Polymer-Plastics Technology and Engineering* **48**, 285–291, 2009.
24. Rao C. R..; The use and interpretation of principal component analysis in applied research. *The Indian Journal of Statistics,* 329-358, 1964.
25. Lias S., Ali N. A. M., Jamil M., et al.; Classification of pure and mixture agarwood oils by electronic nose and discriminant factorial analysis (DFA). *ICSSA* 7–10, 2015.

I PointNet++: Improved PointNet++ for Segmentation and Localization of Leather Grasp Points

by

Guang Jin,[1] Gongchang Ren,[1] Yuan Huan[1] and Jiangong Sun[1]
[1]*College of Mechanical & Electrical Engineering at Shaanxi University of Science & Technology,*
Xi'an, Shaanxi, 710021, China

1 - Abstract

In order to achieve accurate identification and positioning of leather grasp points during the process of robot grasp and spreading leather, this paper proposes a leather grasp point segmentation and positioning method based on improved PointNet++(IPointNet++). Taking leather in its natural falling state as the research object, a depth camera is used to collect point cloud data of the leather. Firstly, the preprocessing of leather point clouds is completed by removing background point clouds based on PassThroughFilter and eliminating noise based on Statistics Filter. Secondly, the octree sampling method is used to replace the farthest point sampling method of the original PointNet++, which is adapted to the non-rigid deformation characteristics of the leather itself. Thereby, the entire leather is divided into two parts: the main body and the grasp area. Lastly, the three-dimensional coordinates of the leather grasp points are obtained by solving the centroid of the point cloud data in the leather grasp area grasp. In the segmentation experiments, the improved PointNet++ has raised the mIoU by 11.8% and 2.5% comparing with PointNet and PointNet++ respectively, and the OA by 6.1% and 1.1%. In the grasp experiments, the success rate of leather grasp points identification grasp is 93.33%, and the success grasp rate grasp is 82.14%. The experimental results show that the proposed method has higher segmentation accuracy and good applicability.

2 - Background

The leather manufacturing industry is an important branch of the light industry and plays a significant role in the manufacturing industry. However, in the current stage, traditional methods are still used for handling and spreading leather in some processes and inter processes, which require a large amount of labor. High labor intensity and poor working conditions still exist in the whole process. The leather processing industry is at the critical period of transformation and upgrading, and it is urgent to solve the key problem of how to combine robot technology to achieve automation in various processes of leather production.

To address the automation of leather operations using robot technology, Huan et al.[1] designed a specifical robotic hand for grasp and spreading leather, and enabled the grasp and spreading operations on the leather by dual robotic arms. However, due to some factors of the leather itself, such as the irregular edges, deformational susceptibility under stress, and easy occlusion caused by bending, furthermore, the influence of external factors such as cluttered backgrounds and lighting changes in the processing environment, the recognition of the grasp area of the leather is a challenging problem during the dual-arm grasp and spreading process.

In order to solve the problem of difficult recognition and positioning of the grasp area and obtaining the corresponding three-dimensional coordinates grasp during the dual-arm grasp and spreading process, this paper uses point cloud data that can reflect spatial information as the foundation and adopts a deep learning-based 3D point cloud segmentation algorithm to recognize and segment the target area,[2-4] thereby the three-dimensional coordinates of the lowest grasp area of the leather is obtained grasp.

3D point cloud segmentation based on deep learning can be divided into indirect and direct methods. Indirect segmentation involves projecting the point cloud into multiple views of 2D images and performing convolutional operations on the projected 2D data to achieve point cloud segmentation. SU et al.[5] proposed MVCNN (multi-view convolutional neural network), which extracts features from 2D images of three-dimensional objects under multiple views, and finally aggregates the 2D images from multiple views through pooling and fully connected operations to obtain the segmentation result. However, this method loses the three-dimensional spatial features of the target, resulting in lower segmentation accuracy. FENG et al.[6] proposed GVCNN (group-view convolutional neural network), which groups the descriptors extracted from 2D images under different views, solving the problem of losing three-dimensional spatial features in MVCNN under multiple views.

Direct segmentation, as a method that directly operates on raw point cloud data, reduces computational complexity and processing errors. QI et al.[7] proposed the PointNet network, which directly processes the data and extracts the feature information of the target from the point cloud data. The core of PointNet is the adoption of Multi-Layer Perceptron (MLP) for feature extraction

Corresponding author email: rengc@sust.edu.cn
Manuscript received November 27, 2023, accepted for publication January 22, 2024.

of each point in the data, and the use of the symmetric function Maxpool to obtain information for each point, which solves the issues of unorderedness, permutation invariance, and rotation invariance of point clouds.[8] However, PointNet does not extract and process local features, without considering the relationships between points and their neighbors. Therefore, QI et al.[9] proposed PointNet++, which uses farthest point sampling (FPS) to define multiple local regions as clusters and selects the centroid of each cluster. By searching for the neighboring points of the centroids, multiple subsets of point clouds are obtained, and the features of these subsets are obtained through convolution and pooling operations. PointNet++ enables better extraction and processing of local features and addresses the issue of uneven sample distribution while considering the relationships between points. Zhao et al. [10] proposed Point Transformer, which is constructed based on the self-attention mechanism[11] model and incorporates position encoding. The proposed method can effectively handle unordered point cloud data and achieve point cloud segmentation by utilizing the mutual relationships between points in local neighborhoods. Indirect segmentation methods suffer from incomplete three-dimensional spatial information, while direct segmentation methods can obtain complete feature information and extract local feature information of the target[12]. Considering the characteristics of leather itself, in order to capture the local feature information of the grasp area of leather better, this study adopts the PointNet++ network. However, the farthest point sampling (FPS) used in PointNet++ cannot adapt to the non-rigid deformation of leather. To segment the leather point cloud better, the original algorithm's FPS method is replaced with octree sampling in this paper, which allows the network to adapt to the characteristics of leather under different grasp states better, the segmentation of leather point cloud data is achieved consequently.

3 - Materials and Methods

This paper proposes an improved PointNet++ point cloud segmentation model, which can segment leather in its natural drooping state and grasp area, and then locates the three-dimensional coordinates of the grasp area based on the segmentation results. The specific process is shown in Figure 1.

3.1 - Data Acquisition

The experiment utilized the Intel RealSense D435i depth camera for data collection. The camera has a resolution of 1280×720 and a depth field of view of 69.4°×42.5°. The camera was positioned 1.5m away from the object and fixed in front of the robotic arm, as shown in Figure 2. The data collection was conducted under conditions with no specific background or lighting, and the leather was grasped by the robotic arm in its natural droop state for 3D point cloud acquisition. Due to the diversity and variability of leather shapes,

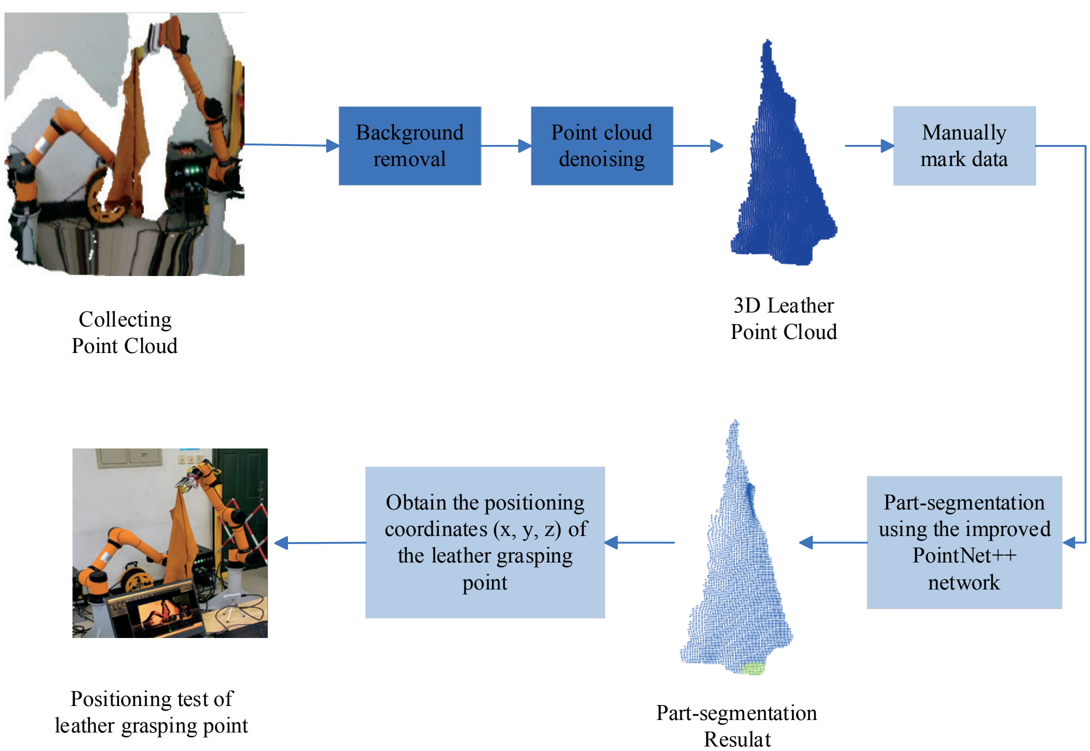

Figure 1. Location process of leather grabbing area based on point cloud information.

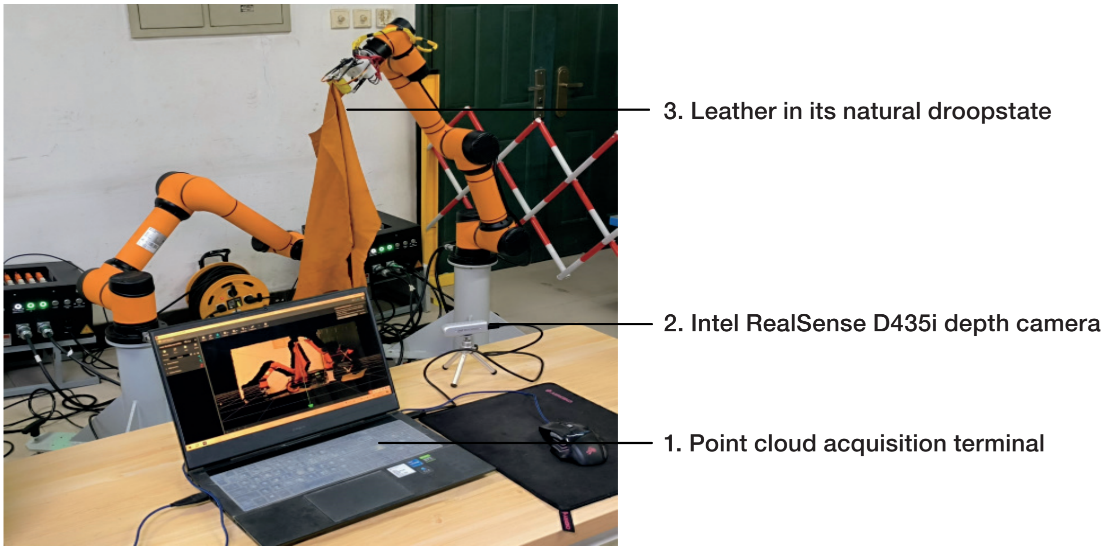

Figure 2. Illustration of leather point cloud acquisition

20 leather samples were selected, and each sample was randomly drooped 10 times, resulting in a total of 200 samples.

3.2 - Point Cloud Preprocessing

During the point cloud data acquisition, background and a certain amount of noise points are inevitably captured. Therefore, appropriate preprocessing operations are performed on the raw point cloud data before segmentation to remove redundancies and improve the training speed of the network. A passthrough filter is applied to remove most of the background, which is followed by a statistical filter to remove noise.

3.2.1 - Background Removal with Passthrough Filter

A passthrough filter was used to remove the background. The threshold values for the X, Y, and Z directions are set to $X \in [-0.25m,\ 0.05m]$, $Y \in [-0.2m,\ 0.6m]$ and $Z \in [-1.8m,\ 1.4m]$ to achieve effective background removal. The filtered result is shown in Figure 3, which demonstrates that the passthrough filter removes most of the background while preserving the relevant information of the leather effectively.

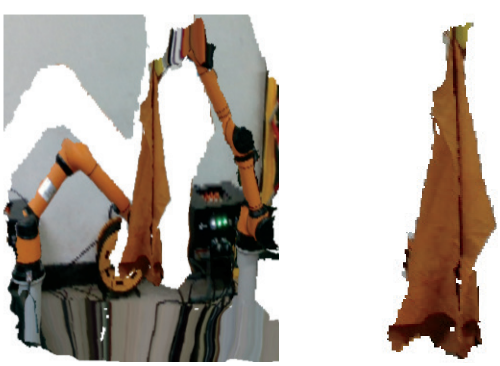

Figure 3. Effect of Passthrough Filter

3.2.2 Statistics Filtering for Noise Removal

Noise points in the point cloud can have a significant impact on the localization of the leather grasp region. Statistics filtering is used to remove noise points around the leather. First, the number of points in the point cloud data, denoted as n, and the number of neighboring points, denoted as m, are calculated. The distance between each point and its neighboring points, denoted as d_{ij}, is computed, where $i = \{1,2\cdots,n\}$ and $j = \{1,2\cdots,m\}$. The distances between all points and their neighboring points are then used to calculate the Gaussian distribution, which has mean distance μ and distance standard deviation σ.

The distance between the i-th point with coordinates $P_i = (X_i,\ Y_i,\ Z_i)$ and any neighboring point $P_j = (X_j,\ Y_j,\ Z_j)$ is calculated using the following formula:

$$d_{ij} = \sqrt{(X_i - X_j)^2 + (Y_i - Y_j)^2 + (Z_i - Z_j)^2} \quad (1)$$

The mean distance μ and distance standard deviation σ for each point to its neighboring points are calculated by iterating through the point cloud, using the following formulas:

$$\mu = \frac{1}{n}\sum_{i=1}^{n} d_{ij} \quad (2)$$

$$\sigma = \sqrt{\frac{1}{n}\sum_{i=1}^{n} (d_{ij} - \mu)^2} \quad (3)$$

Noise points are removed when the condition $\mu - \omega\sigma < d_{ij} < \mu + \omega\sigma$ (where ω is a multiple of the standard deviation) is met. Through experiments, it has been found that m = 20 and ω = 0.8 can effectively remove noise points around the leather, as shown in Figure 4.

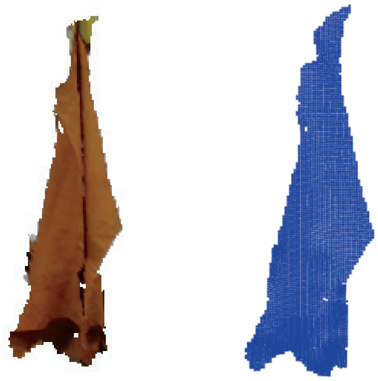

Figure 4. Point cloud data before and after statistical filtering

Figure 5. Segmentation diagram of the leather grasp region

3.3 - Data Labeling

Based on the analysis of the operation process of leather grasp and spreading by the dual robotic arm, it is necessary to identify the lowest corner points of the leather. Therefore, the leather needs to be divided into two parts: the leather body and the grasp region. The segmentation diagram is shown in Figure 5.

In the process of deep learning point cloud segmentation, the training set needs to be manually labeled. Due to the inherent characteristics of leather and the influence of external environmental factors, the grasp region of the leather in its natural droop state may exhibit concave and up wrap phenomena. Therefore, the lowest corner point of the leather is used for labeling the grasp region. The data set is labeled into two categories, with the leather body as "0" and the grasp region as "1". The specific labeling process is shown in Figure 6.

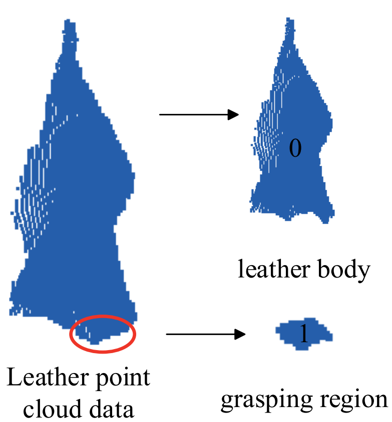

Figure 6. Partial manual labeling of leather point cloud

4 - Improvement of the PointNet++ Model (I PointNet++)

Octree sampling is a top-down progressive spatial partitioning structure. In order to address the flexible deformation characteristics of leather, octree sampling is used to process the point cloud data systematically, which can achieve a good topological relationship of the unordered point cloud data and enable k-nearest neighbor search for feature points.

The leather point cloud was divided using octree sampling. Firstly, the parent node of the preprocessed leather point cloud was determined. Then, the parent node was divided into eight sub-nodes along the directions of the spatial coordinate system. Each octree node represents a cube, and each parent node was divided into eight sub-nodes. All nodes were subdivided into eight equal parts until the side length of the cube was smaller than the set threshold, when the partitioning terminated. The illustration of octree partitioning is shown in Figure 7.

The IPointNet++ network structure is shown in Figure 8. It takes a preprocessed single leather point cloud data [*npoint* × 3] as input, where npoint is the number of points in the point cloud and 3 represents the point cloud coordinates (X, Y, Z). The leather point cloud was sampled and divided based on the feature points obtained from octree sampling. The octree has 5 layers, and the number of center points for sampling is n_1. The neighborhood of center points (nsample) is $n_2 = 64$. The local point clouds sampled and grouped by PointNet layers were encoded to obtain feature vectors of size (1024, 256). The octree sampling, grouping, and encoding of local point

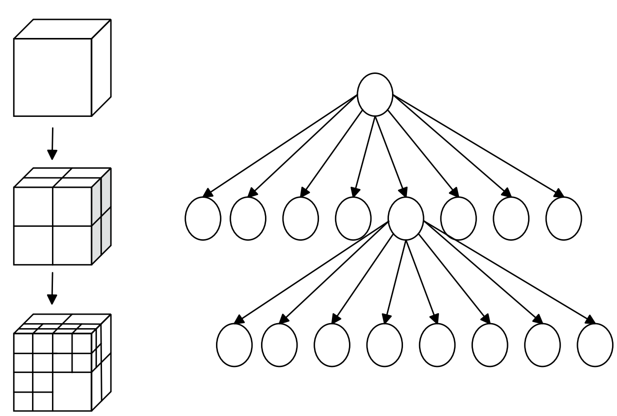

Figure 7. Illustration of octree partitioning

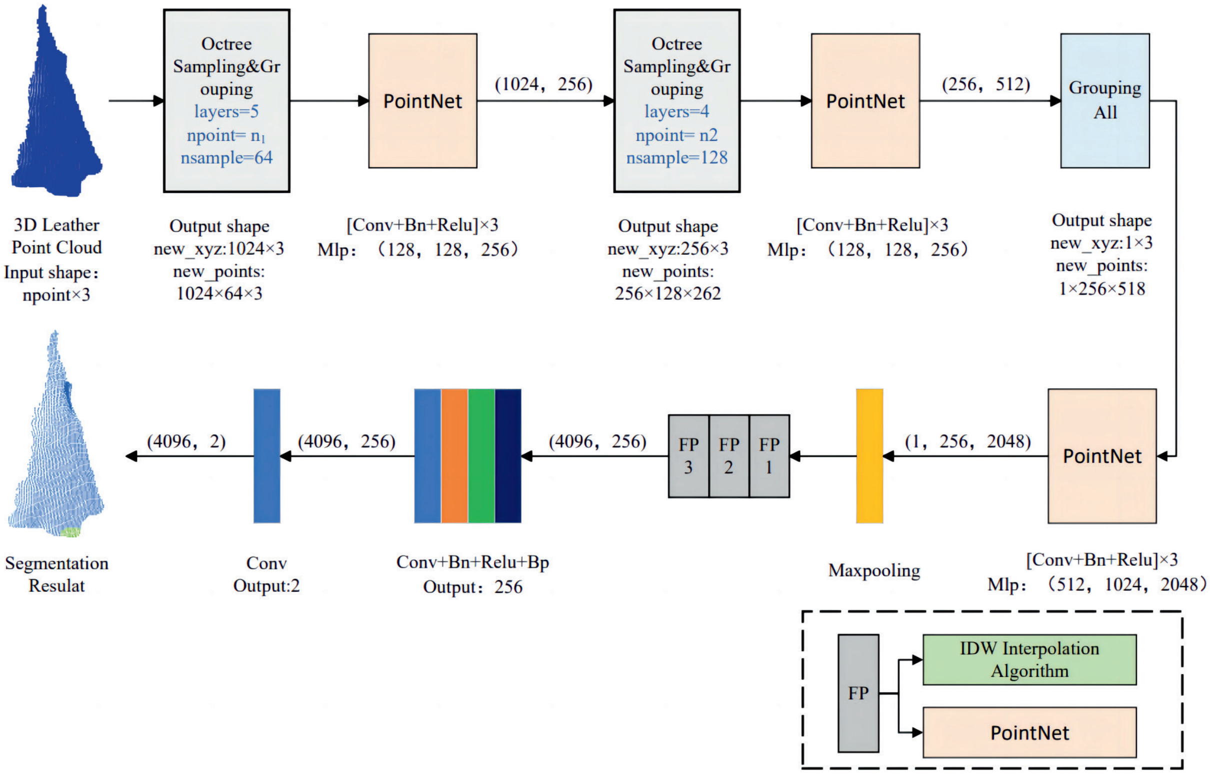

Figure 8. Schematic diagram of IPointNet++

clouds were repeated, resulting in feature vectors of size (256, 512). In this case, the octree has 4 layers and the number of neighborhood points for center points is n_2. The feature vectors were then encoded by PointNet layers. After undergoing max pooling and three FP (Feature Propagation) layers, where the FP layers involve Inverse Distance Weighted (IDW) interpolation algorithm and PointNet operations, the feature vectors of size (4096, 256) were obtained. The IDW interpolation formula is as follows:

$$f^{(i)}(x) = \frac{\sum_{i=1}^{k} w_i(x) f_i^{(j)}}{\sum_{i=1}^{k} w_i(x)} \tag{4}$$

$$w_i(x) = \frac{1}{d(x,x_i)^p} \tag{5}$$

Where f represents the interpolated feature value, $d(x, x_i)$represents the distance, p represents the index, k is the number of neighborhood points, and $j=1,2,\cdots,C$.

The obtained feature vectors of size (4096, 256) were then passed through a Conv+Bn+Relu+Bp (Convolution + Batch Normalization + Activation Function + Backpropagation) layer, the two classes of feature points (leather body and leather grasp region) was obtained by one Convolution operation grasp. The maximum value was taken as the output result for segmenting the leather point cloud. Point cloud segmentation is a classification problem for each segmentation point, the Cross Entropy Loss function was used as the loss function for the network model, with the formula as follows:

$$\text{Loss} = -\frac{1}{N}\sum_{i=0}^{N-1}\sum_{k=0}^{K-1} y_{i,k} \ln p_{i,k} \tag{6}$$

Where $y_{i,k}$ represents the true label of sample i as k, with K label values and N samples, and $p_{i,k}$ represents the predicted label value for sample i as k.

5 - Localization of Leather Grasp Points

During the process of leather grasp point localization, the opening range of the robotic hand is 15cm. To ensure reliable grasp, the centroid of the leather grasp region is selected as the optimal grasp point. As shown in Figure 9, O-XYZ represents the spatial coordinate system of the target.

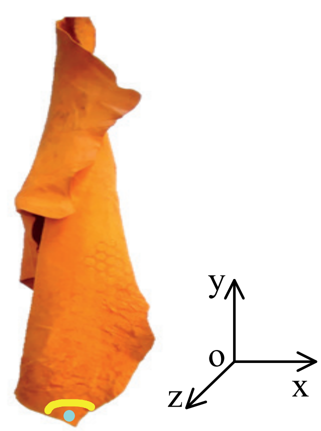

Figure 9. Coordinate system of the target

The formula for calculating the centroid of the leather grasp region is as follows:

$$P_c = \sum_{i=0}^{n} m_i r_i \quad (7)$$

where m_i represents the mass of the point cloud, $r_i = (x_i, y_i, z_i)$ and m_i is set to 1. Therefore, the formula for the centroid coordinates of the point cloud is as follows:

$$P_c\,(x_c, y_c, z_c) = \frac{1}{n}(\sum_{i=0}^{n} x_i, \sum_{i=0}^{n} y_i, \sum_{i=0}^{n} z_i \quad (8)$$

where n represents the number of points in the point cloud, and $i = \{1, 2, ..., n\}$.

6 - Experimental Process and Result Analysis

6.1 - Experimental Conditions

The experiments were conducted in a Windows 11 operating system environment, using the Pytorch framework. For the localization experiments, the Intel RealSense D435i depth camera was used to capture the leather point cloud, and the AUBO-i5 dual-arm robot was used for the grasp localization experiments. The specific experimental configuration is shown in Table I.

6.2 - Segmentation Experiment

6.2.1 - Experimental Design

To verify the effectiveness of the proposed algorithm, comparative experiments were conducted on the IPointNet++ algorithm, the original PointNet algorithm, and the original PointNet++ algorithm under the same conditions which includes training data, number of iterations, optimizer, learning rate, batch size, and training device. The training parameters were set as shown in Table II.

The average ratio of the intersection to the union of predicted values and true values for each category is represented by mIoU. The formula is as follows:

$$\text{mIOU} = \frac{1}{N}\sum_{i=0}^{N}\frac{p_{ii}}{\Sigma_{j=0}^{N} pij + _{j=0}^{N} pij - pij} \quad (9)$$

OA represents the ratio of correctly classified point clouds to the total number of point clouds. The formula is as follows:

$$\text{OA} = \frac{\Sigma_{i=0}^{N} p_{ii}}{\Sigma_{i=0}^{N}\Sigma_{j=0}^{N} pij} \quad (10)$$

where N represents the number of categories in the point cloud dataset, p_{ii} represents the correctly predicted point clouds for a category, p_{ij} represents the incorrectly predicted point clouds for a

Table I

Experimental configuration

Parameters	Configuration
Operating System	Windows 11
Graphics Memory	12GB
RAM	64GB
GPU	NVIDIA GeForce RTX 3060
GPU Acceleration Environment	CUDA11.3
Training Framework	Pytorch
Programming Language Environment	Python 3.9
Depth Camera	Intel RealSense D435i
Dual Robotic Arms	AUBO-i5

Table II

Training parameter settings

Parameters	Value
epochs	200
batch-size	16
Learning rate	0.001
Attenuation rate	0.5

Evaluation metrics: Mean Intersection over Union (mIoU) and Overall Accuracy (OA).

category, and p_{ij} represents the point clouds of category *j* predicted as category *i*.

6.2.2 - Results and Analysis

The obtained training results are shown in Table III. Compared with the PointNet algorithm, the IPointNet++ algorithm has enhanced mIoU by 11.8% and OA by 6.1%. Compared with the original PointNet++ algorithm, the IPointNet++ algorithm has enhanced mIoU by 2.5% and OA by 1.1%. From the results of the model training, it can be seen that the performance of the IPointNet++ algorithm has been improved greatly, and the effectiveness of the proposed algorithm has been validated. The proposed IPointNet++can provide leather grasp point recognition and segmentation for subsequent grasp localization experiments.

To further validate the applicability and feasibility of the proposed algorithm, unsampled leather was selected for verification. As shown in Figure 10, when facing different leather point cloud samples, it can be seen that the proposed algorithm can still effectively segment the leather into the main body and the leather grasp region accurately and clearly.

To evaluate the comprehensive segmentation capability of the proposed algorithm further, a comparison was made with the PointNet algorithm and the original PointNet++ algorithm for the segmentation task using unsampled leather. The segmentation results of the three algorithms are shown in Figure 11. It can be observed that the IPointNet++ algorithm can effectively segment the leather precisely and accurately, which can meet the subsequent localization of leather grasp regions. Due to its inability to adapt well to the non-rigid deformation, the original PointNet++ algorithm segments the grasp region of the leather into a larger area, which can lead to excessive segmentation of the grasp region, which will affect the localization accuracy of the leather grasp points. The PointNet algorithm shows either small or incorrect segmentation results for the leather, ascribing to its inability to handle the relationships between points and their neighbors well, and cannot perform local feature extraction which can greatly affect the localization of the grasp region and processing specifically for the leather grasp.

6.3 - Grasp Localization Experiment

To verify the effectiveness of the proposed localization algorithm, the three-dimensional coordinates of the segmented leather grasp

Table III

Segmentation accuracy results (%)

Model	mIoU	OA	Single-Class Classification	
			Leather Main Body	Leather Grasp Region
PointNet	70.8	89.2	92.3	89.6
PointNet++	80.1	94.2	95.1	92.7
Improved PointNet++	82.6	95.3	96.2	93.1

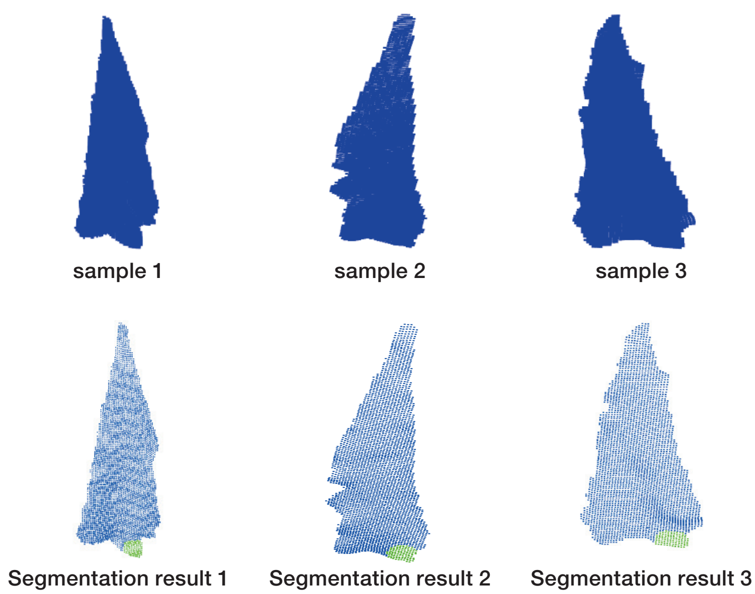

Figure 10. Segmentation results of unsampled leather point cloud

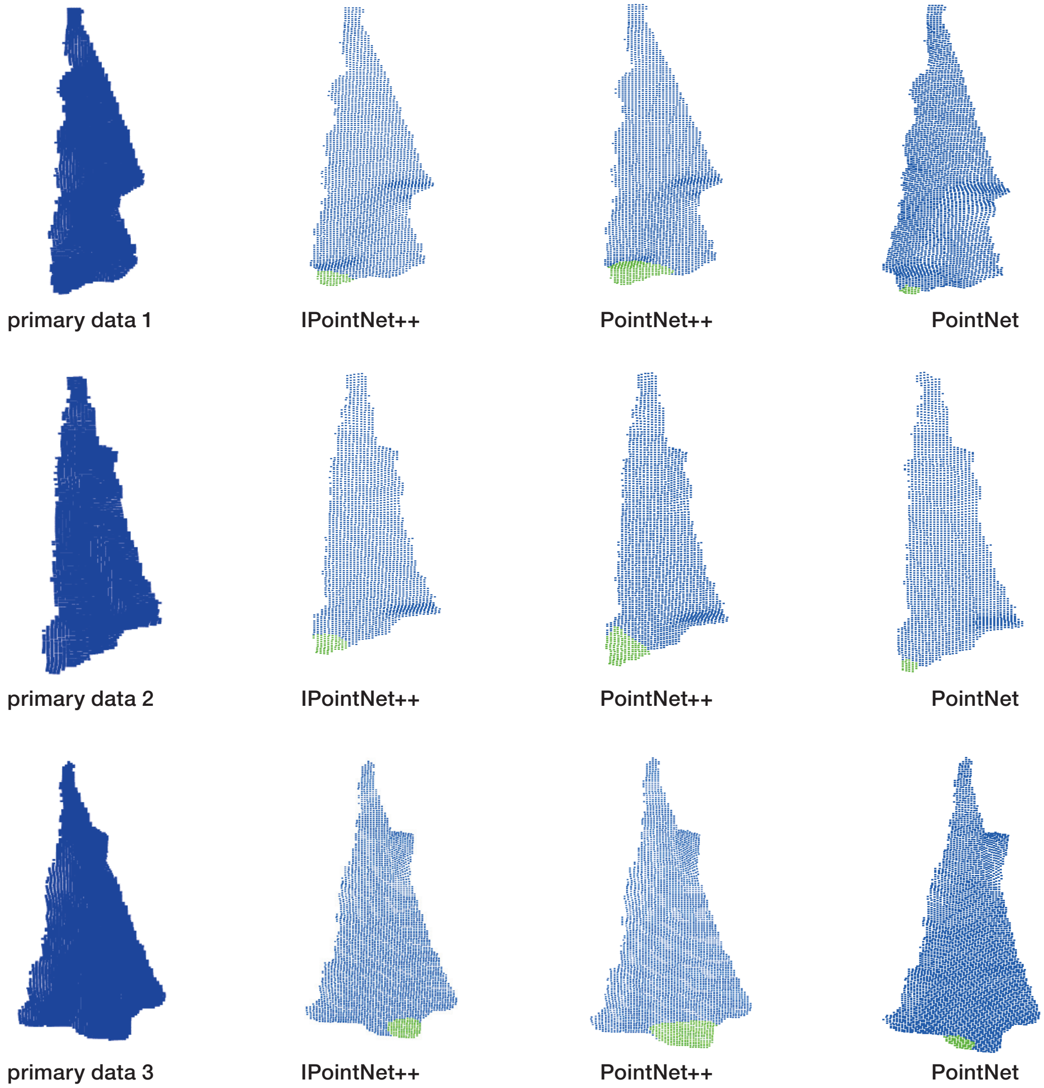

Figure 11. Comparison of segmentation results using different algorithms

region centroids were passed to the robotic arm for the leather grasp. The check whether it could accurately grasp the leather based on the input coordinate values was tested. Thirty random leather samples were selected for the experiment, and the leather was placed on the test bench. The robotic arm was used to grasp the leather and place it in a natural drop state. Then, the proposed algorithm was used to recognize and segment the leather grasp region, and the three-dimensional coordinates of the leather grasp region centroid were obtained. The coordinates were then passed to another robotic arm to check whether it could accurately grasp the leather grasp point.

Evaluation metrics: The success rate, which was calculated as the ratio of the successful grasp number to the total experimental number.

6.3.1 - Results and Analysis

The overall experimental process is shown in Figure 12.

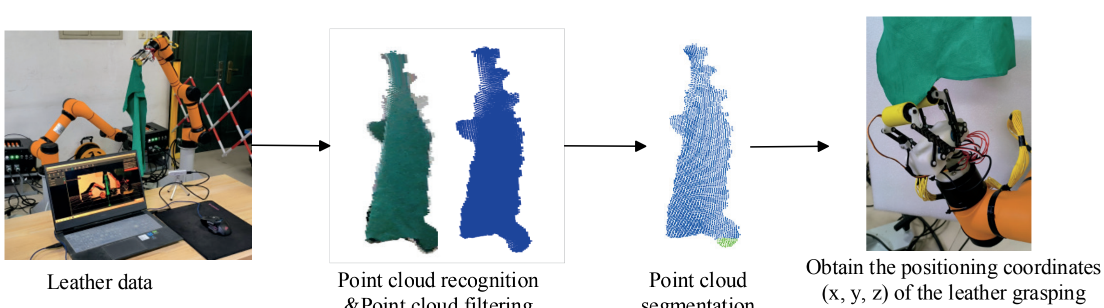

Figure 12. Overall experimental process

Table IV

Test data for grasp localization experiment

Identification experiment/times	Successful identification/times	Failure identification/ times	Success rate/%
30	28	2	93.33
Grab experiment/times	Successfully grabbed/ times	Failed fetching/times	Success rate/%
28	23	5	82.14

The test data is shown in Table IV.

According to Table IV, for the 30 experiments, the leather grasp points were successfully recognized 28 times, with a success rate of 93.33%. The result showed that the recognition success rate was affected by the defects (damage, rough edges) of the leather which can lead to recognition errors and inability to segment the leather grasp region. The total number of grasp attempts was 28 times, with 23 successful grasp and a success rate of 82.14%. The analysis showed that the grasp success rate was affected by factors which can make it difficult to accurately grasp the leather grasp point such as the recognition success rate, the grasp posture of the robotic arm, and the opening angle of the robotic arm. In summary, the proposed algorithm can meet the recognition, segmentation, and localization of leather grasp points better, but future research is still needed to determine the optimal grasp posture and opening angle of the robotic arm to improve the overall grasp success rate furtherly.

7 Conclusion

To achieve the segmentation and localization of leather grasp points during the grasp process, the IPointNet++ was proposed in this paper, which replaced the farthest point sampling method of the original PointNet++ algorithm with the octree sampling method, achieved segmentation of the leather that is prone to non-rigid deformation, obtained the leather grasp region, calculated the centroid of the leather grasp point, obtained the three-dimensional coordinates of the grasp point and grasped the leather using a dual-arm robot.

1. In the segmentation experiment, the proposed IPointNet++ algorithm increased the MIoU by 2.5% and the OA by 1.1% compared with the original PointNet++ algorithm.

2. In the grasp localization experiment, the recognition success rate of the leather grasp points was 93.33%, and the grasp success rate was 82.14%. The Analysis showed the grasp posture and opening angle of the robotic arm are the main factors which can affect the grasp success rate.

In summary, the proposed IPointNet++ algorithm can recognize, segment, and locate leather grasp points effectively, which has significant implications for advancing the use of robots in leather processing.

Data availability
The data that support the findings of this study are available from the corresponding author upon reasonable request.

Author contributions
GJ and YH conceptualized the project, developed the methodology, prepared the original draft, and carried out the experiments. GR supervised the project and was responsible for the project administration. JS assisted in the experiment. All the authors have read and agreed to the published version of the paper.

Competing interests
The contact author has declared that none of the authors have any competing interests.

Financial support
This research has been supported by Xi'an Science and Technology Plan Project (grant no. 23ZDCYJSGG0016-2022) and Shaanxi Provincial Key R&D Program Funding Project (grant no. 2022GY-250).

References

1. Huan, Y.; Ren, G.; Su, X.; Tian, W., A versatile end effector for grabbing and spreading of flaky deformable object manipulation. *Mech. Sci.* **2023,** *14* (1), 111-123.
2. Rusu, R. B.; Marton, Z. C.; Blodow, N.; Dolha, M.; Beetz, M., Towards 3D Point cloud based object maps for household environments. *Robotics and Autonomous Systems* **2008,** *56* (11), 927-941.
3. Li, J.; Chen, B. M.; Lee, G. In *SO-Net: Self-Organizing Network for Point Cloud Analysis*, 2018 IEEE/CVF Conference on Computer Vision and Pattern Recognition (CVPR), 18-23 June 2018; 2018; pp 9397-9406.

4. Zhao, H.; Jiang, L.; Fu, C. W.; Jia, J., Pointweb: Enhancing local neighborhood features for point cloud processing. In *Proceedings of the IEEE Computer Society Conference on Computer Vision and Pattern Recognition*, 2019; Vol. 2019-June, p 5560.
5. Su, H.; Maji, S.; Kalogerakis, E.; Learned-Miller, E. In *Multi-view Convolutional Neural Networks for 3D Shape Recognition*, 2015 IEEE International Conference on Computer Vision (ICCV), 7-13 Dec. 2015; 2015; pp 945-953.
6. Feng, Y.; Zhang, Z.; Zhao, X.; Ji, R.; Gao, Y. In *GVCNN: Group-View Convolutional Neural Networks for 3D Shape Recognition*, 2018 IEEE/CVF Conference on Computer Vision and Pattern Recognition, 18-23 June 2018; 2018; pp 264-272.
7. Charles, R. Q.; Su, H.; Kaichun, M.; Guibas, L. J. In *PointNet: Deep Learning on Point Sets for 3D Classification and Segmentation*, 2017 IEEE Conference on Computer Vision and Pattern Recognition (CVPR), 21-26 July 2017; 2017; pp 77-85.
8. Mao, J.; Wang, X.; Li, H. In *Interpolated Convolutional Networks for 3D Point Cloud Understanding*, 2019 IEEE/CVF International Conference on Computer Vision (ICCV), 27 Oct.-2 Nov. 2019; 2019; pp 1578-1587.
9. Qi, C. R.; Yi, L.; Su, H.; Guibas, L. J., PointNet++: deep hierarchical feature learning on point sets in a metric space. In *Proceedings of the 31st International Conference on Neural Information Processing Systems*, Curran Associates Inc.: Long Beach, California, USA, 2017; pp 5105–5114.
10. Zhao, H.; Jiang, L.; Jia, J.; Torr, P.; Koltun, V. In *Point Transformer*, 2021 IEEE/CVF International Conference on Computer Vision (ICCV), 10-17 Oct. 2021; 2021; pp 16239-16248.
11. Vaswani, A.; Shazeer, N.; Parmar, N.; Uszkoreit, J.; Jones, L.; Gomez, A. N.; Kaiser, L.; Polosukhin, I., Attention Is All You Need. *arXiv e-prints* **2017**, arXiv:1706.03762.
12. Li, Y.; Bu, R.; Sun, M.; Wu, W.; Di, X.; Chen, B., PointCNN: convolution on X-transformed points. In *Proceedings of the 32nd International Conference on Neural Information Processing Systems*, Curran Associates Inc.: Montréal, Canada, 2018; pp 828–838.

Examination of Haloversatile Bacteria on Salted Goatskin and Inactivation of Haloversatile Bacteria via Direct Electric Current

by
S. Kose,[1] P. Yilmaz,[2]* M. Birbir[2] and Y. Birbir[3]
[1]*Marmara University, Institute of Pure and Applied Sciences,* Ziverbey, 34722, Istanbul, Türkiye
[2]*Marmara University, Faculty of Science, Department of Biology, Division of Plant Diseases and Microbiology,* Ziverbey, 34722, Istanbul, Türkiye
[3]*Marmara University, Technology Faculty, Electric and Electronic Engineering Department,* Ziverbey, 34722, Istanbul, Türkiye

Abstract

Haloversatile bacteria are among the commonly found microorganisms that have the potential to damage hides and skins in the leather industry. Therefore, the objective of this study was to investigate the presence of haloversatile bacteria on salted goatskins, to characterize these microorganisms through the use of molecular and conventional test methods, to detect their impact on the skins, and finally find an effective solution to inactivate these microorganisms. Haloversatile bacteria were common inhabitants at salted goatskin samples obtained from the Tuzla Organized Leather Industry Zone in Türkiye. Total numbers of haloversatile bacteria, proteolytic haloversatile bacteria, and lipolytic haloversatile bacteria on ten salted goatskin samples ranged from 7×10^4 to 2.7×10^5 CFU/g, 1×10^4 to 8×10^4 CFU/g, and 1×10^4 to 1.3×10^5 CFU/g, respectively. In the present study, 88% of the isolates were protease-positive, 69% were lipase-positive, 8% were xylanase-positive, 27% were caseinase-positive, 23% were amylase-positive, 8% were DNase-positive, 31% were cellulase-positive, 54% were urease-positive, 100% were catalase-positive, and 54% were oxidase-positive. The bacterial isolates showed positive reactions for the utilization of different amino acids such as glycine, L-cysteine, L-proline, and L-threonine, having the highest rates of 88%, 80%, 80%, and 80%, respectively. However, L-histidine had a lower positive reaction rate of 31%. The halophilic bacterial isolates exhibited positive reactions for the utilization and acid production from different types of sugar, with glucose having the highest positive reaction rate of 81%, followed by maltose at 73%, xylose at 58%, galactose at 46%, and lactose at 42%. Haloversatile enzyme-producing bacteria were identified using biochemical and molecular methods, resulting in the identification of 17 different species. Micrographs obtained from the scanning electron microscope revealed the damage inflicted on the fresh goatskin structure by haloversatile bacteria. A direct electric current of 2.2 A was applied to the mixed culture of haloversatile bacteria for 25 minutes to find an effective inactivation method. The total count of the mixed culture of haloversatile bacteria decreased from 7.3×10^6 CFU/mL to 4 CFU/mL within 16 minutes. All seventeen haloversatile bacteria in the mixed culture were killed within 19 minutes.

Introduction

The leather industry plays a significant role in the global economy by utilizing waste products from the meat industry to produce durable and valuable commercial products. Especially the longevity of leather products makes them a sustainable choice compared to some synthetic alternatives. Different leather goods such as footwear, jacket, bag, shoe, wallet, and garment are produced by animal skins and hides.[1,2] Due to the presence of proteins (collagen, glycoproteins, keratin, elastin, globulins and albumins), carbohydrates, lipids, mineral salts and water in animal hides and skin microorganisms can grow on the raw hides and skins.[3,4] The contamination of brine cured hides, salted hides, salted sheepskins, salted goatskins, and preservation salt with extremely halophilic archaea,[5] moderately halophilic bacteria,[5,6,10-14] halotolerant bacteria,[15-19] and fungal species[20] were previously reported. The metabolic activities of these microorganisms cause grain peeling, hair slip, bad odor, loose grain break, grain sueding, disintegration of the structure of raw skins and hides.[5,15,17,21] In this regard, the destructive effects of microorganisms may cause major economic loss in the leather industry.

Although there are studies reporting the presence of halotolerant bacteria,[15-19] moderately halophilic bacteria,[5,6,10-14] extremely halophilic archaea[5-9]and fungi[20] in brine cured hides, salted hides, salted sheepskins, salted goatskins, and preservation salt, haloversatile bacteria found in salted goatskin samples in the leather industry have not been searched.

Previous study showed that haloversatile bacteria were also the other microorganisms found in the leather industry. It was reported that haloversatile *Terribacillus halophilus*, *Brevibacterium luteolum*, *Bacillus australimaris*, *Bacillus siamensis*, and *Bacillus mojavensis* species were isolated from soak liquor samples of leather industry.[22]

While haloversatile bacteria can grow the medium with NaCl and the medium containing up to 3M NaCl, optimum NaCl concentrations for haloversatile bacteria are 0.2-0.5 M NaCl.[23,24] The ability of accumulation compatible solutes allows haloversatile bacterial cells to survive under high osmotic stress.[25,26] Cold-

*Corresponding author e-mail: pinar.caglayan@marmara.edu.tr
Manuscript received November 23, 2023, accepted for publication January 14, 2024.

loving haloversatile bacterial species (*Carnobacterium funditum*, *Methanococcoides burtonii*, *Halomonas meridiana*, *Halobacterium lacusprofundi*, *Flavobacterium salegens*, *Carnobacterium alterfunditum*, *Halomonas subglaciescola*, *Flectobacillus glomeratus*, *Flavobacterium gondwanense*, *Vesiculatum antarcticum*) obtained from seawater of Antarctica were firstly reported by Ellis-Evans in 1985.[27] The production of compatible solutes by a haloversatile, psychropiezophile deep-sea bacterium *Photobacterium profundum* (isolate code SS9) was also stated.[28] Kaye et al. (2011)[29] studied the biodiversity of haloversatile *Marinobacter* species in seawater to investigate their biotechnological importance. Two haloversatile isolates which were obtained from mangroves in the Red Sea were reported by the researchers.[30]

The haloversatile bacterial strains belonging to the genus *Bacillus*, *Kocuria*, *Paracoccus*, *Micrococcus*, *Microbacterium*, *Brevibacterium*, *Staphylococcus*, *Acinetobacter*, *Exiguobacterium*, *Gordonia*, *Microbacterium*, *Pseudomonas*, *Agrococcus*, *Sanguibacter*, *Virgibacillus*, *Rhodococcus*, *Marinobacter*, *Vibrio*, *Marinomonas Salinivibrio* were isolated from salt and brine samples of Camalti Saltern.[31,32] The salt obtained from Camalti Saltern is also used in the leather industry to preserve hides and skins. The presence of proteolytic and lipolytic haloversatile bacteria in curing salt may cause contamination of salted hides and skins. To prevent the damage of salted hides and skins due to these microorganisms is very important. In 2006, Birbir and Birbir detected that low-level direct electric current was highly effective in inactivating various species of extremely halophilic archaea that were isolated from salt samples. The researchers reported that this technique could be used in the leather industry.[33] Direct electric current[9,33-35] and combined application of alternating and direct electric currents[36-40] were used for inactivating of different microorganisms found on the samples collected from the leather industry. Also, fresh orange juice,[41] drinking water[42] and seawater[43] were treated with direct electric current to control microorganisms. The inactivation of bacteria and archaea by direct electric current has garnered significant interest due to its high efficiency, cost-effectiveness, and applicability.

Although the presence of haloversatile bacteria in sea water,[27,29] mangroves in the Red Sea,[30] salt and saltern[31,32] and soak liquor[22] was previously reported by few researchers, the presence of the haloversatile bacteria in the salted goatskin samples were not reported yet. Hence, the aims of the present study were to collect salted goatskin samples from the Tuzla Leather Organized Industrial Zone (Istanbul, Türkiye); to detect the total number of haloversatile bacteria, the total numbers of proteolytic and lipolytic haloversatile bacteria on the salted goatskin samples; to identify haloversatile bacterial isolates with conventional and molecular methods; to examine the damage caused by haloversatile bacteria on the fresh goatskin using Scanning Electron Microscope and to inactivate these isolates via direct electric current treatment.

Experimental

Collection of Salted Goatskin Samples from Tanneries and Measurement of pH Values

In this study, ten salted goatskin samples were obtained from the tanneries in the Tuzla Leather Organized Industrial Zone (Istanbul, Türkiye) and placed in sterile bags. Subsequently, the goatskin samples were placed in an insulated box with ice and they were immediately transported to the laboratory. To determine pH of salted goatskin samples, 20 grams of each sample were put into Erlenmeyer flasks containing 180 mL of sterilized sodium chloride solution (1.17% w/v). The Erlenmeyer flasks were placed into a shaking incubator for one hour at 90 rpm at 20°C. After this period, pH values were measured with pH-meter (PT 10, Sartorius Professional Meter PP-50 AG, Göttingen, Germany).[44]

Determination of the Total Numbers of Haloversatile Bacteria, Proteolytic, and Lipolytic Haloversatile Bacteria on the Salted Goatskin Samples

To determine the total number of haloversatile bacteria found on salted goatskin samples, 20 grams of each salted goatskin sample were placed into Erlenmeyer flasks containing 180 mL of sodium chloride solution (1.17%, w/v). Then the Erlenmeyer flasks were put into a shaking incubator for one hour at 20°C, 90 rpm. The total numbers of haloversatile bacteria on the salted goatskin samples were determined by using spread plate technique on Halophilic Agar Medium (HAM) containing 11.7 g NaCl, 1 g $MgSO_4.7H_2O$, 0.36 g $CaCl_2.2H_2O$, 5 g protease peptone, 2 g KCl, 0.23 g NaBr, 1 g glucose, 10 g yeast extract, 0.06 g $NaHCO_3$, 20 g agar, 100 µL FeCl trace element, and 1000 mL distilled water.[31] Direct and serial dilutions of bacterial suspensions (10^{-1}-10^{-6}) were spread on the surface of HAM. After inoculation, the Petri dishes were incubated at 35°C for 24 hours. After the incubation period, the haloversatile bacterial colonies grown on HAM were counted. The bacterial suspensions were also spread on the surface of Gelatin Agar Medium (GAM) containing 2% gelatin (w/v) and 1.17% NaCl to determine the total number of proteolytic haloversatile bacteria of the salted goatskin samples. After 24 hours of incubation at 35°C, Frazier's reagent was poured over the bacterial colonies grown on GAM. The presence of transparent zones around the bacterial colonies indicated positive protease activity. Protease-positive bacterial colonies were counted.[11,31,45] To determine the total number of lipolytic haloversatile bacteria of the salted goatskin samples, the bacterial suspensions were spread on Tween 80 Agar Medium (TAM) containing 5 g yeast extract, 11.7 g NaCl, 10 mL Tween 80, 20 g agar, and 1000 mL of sterile distilled water. The plates were incubated at 35°C for 24 hours. Lipase activity was indicated by the presence of opaque zones around the bacterial colonies grown on TAM. Lipase-positive colonies were counted.[45] Colony-forming units (CFU) were used to calculate the quantity of viable bacterial cells in the samples. The pH of all test media was adjusted to 7.0.

Isolation of Haloversatile Bacteria

Twenty grams of each salted goatskin sample were added into 180 mL of sterile physiological saline solution containing 1.17% NaCl. The suspensions were shaken in a shaking incubator at 35°C, 90 rpm for one hour. The direct and serial dilutions (10^{-1}-10^{-6}) were prepared using sterile physiological saline solution (1.17% NaCl). To isolate haloversatile bacteria, 100 µL of bacterial dilution spread over Petri dishes containing HAM. The inoculated Petri dishes were incubated in an incubator at 35°C for 24 hours. After the incubation period, each bacterial colony which was grown on HAM was picked with sterile loops using streak plate technique until pure haloversatile bacterial colonies were obtained.[46,47]

Haloversatile Bacterial Identification

The DNA isolation process of haloversatile bacteria obtained from salted goatskin samples was carried out using the QIAamp DNA Mini Kit (Qiagen) DNA isolation kit.[48] The forward primer 16F27 (5'-AGAGTTTGATCMTGGCTCAG-3') and the reverse primer 16R1488 (5'-CGGTTACCTTGTTAGGACTTCACC-3') were used for the bacterial identification.[49] Subsequently, amplification was carried out using the Polymerase Chain Reaction (PCR) Technique. The 16S rRNA products were purified using the QIAquick PCR Purification Kit (Qiagen). After the 16S rRNA sequence analyses of the isolates, our isolates were identified using the 16S rRNA sequence database on the NCBI website.

Nucleotide Accession Numbers

The 16S rRNA gene sequence data of the isolates reported in this article, namely S1a, S1b, S2a, S2b, S2c, S3a, S3b, S3c, S4a, S4b, S4c, S4d, S5a, S5b, S6a, S6b, S6c, S7a, S7b, S8a, S8b, S8c, S9a, S10a, S10b, and S10c have been submitted to the NCBI and GenBank nucleotide sequence databases under the respective accession numbers: OR835202, OR835208, OR835209, OR835214, OR835215, OR835216, OR835217, OR835218, OR835220, OR835221, OR835222, OR835223, OR835224, OR835227, OR835225, OR835229, OR835230, OR835231, OR835234, OR835233, OR835238, OR835237, OR835239, OR835240, OR835241, OR835242.[50]

Determination of Optimal Growth Conditions for Haloversatile Bacteria

To determine the optimal growth conditions for haloversatile bacteria were determined at different salt concentrations (0%, 1.17%, 2%, 3%, 5%, 8%, 10%, 12%, 15%, 17.5%, 20%, 22.5%, 25% NaCl), at different temperature values (4°C, 10°C, 15°C, 20°C, 25°C, 35°C, 37°C, 40°C, 45°C, 50°C, 55°C, 60°C), and at pH different values (4.0, 5.0, 6.0, 7.0, 8.0, 9.0, 10.0, 11.0, 12.0).[31] The pH of Halophilic Media were adjusted using 1N HCl and 1N NaOH. After inoculation, the Petri plates prepared with different salt concentrations and different pH values were incubated at 35°C for 24 hours.[31] At the end of the incubation period, the optimal conditions for each isolate were recorded.[31]

Investigation of Enzymatic Properties of Haloversatile Bacteria

Cellulase activity was determined using agar-based cellulose media containing 10% NaCl and carboxymethyl cellulose. Bacteria were streaked onto the cellulose media. After the incubation period, bacterial colonies on the cellulose media were stained with a 0.1% congo red solution for 30 minutes and then washed with a 1 M NaCl solution. Positive cellulase activity was indicated by the presence of a clear zone around the bacterial colonies.[51,52] Xylanase activity was assessed by streaking isolates onto sterile xylan media. After the incubation process, the presence of a clear zone around the colonies was considered as a positive indication of xylanase activity.[45] Urease activity was determined using a Urea Agar medium containing phenol red as an indicator. Isolates were streaked onto the media. The development of a pink color in the agar medium after incubation was considered as a positive indication of urease activity.[45] Protease activity was assessed by streaking isolates onto sterile Gelatin Agar media. After the incubation process, the media was overlaid with enough Frazier reagent to cover the Petri dish's surface. Clear zones observed around the colonies were accepted as a positive indication of protease activity.[45] Caseinase activity was assessed by streaking isolates onto sterile Casein Agar media. After the incubation process, the presence of a clear zone around the colonies was evaluated as a positive indication of caseinase activity.[45] DNase activity was determined by streaking isolates onto sterile DNase media. Then, a few drops of 1 N HCl were added to the media. The formation of a clear zone around the colonies showed positive DNase activity.[45] Oxidase test was performed by streaking pure bacterial colonies from the media onto filter paper soaked with para-aminodimethylaniline monohydrochloride. The development of a blue-purple color within 5-10 seconds was considered a positive result.[46,53] Catalase activity was determined by adding a few drops of 3% hydrogen peroxide (H_2O_2) onto pure colonies grown on the media. The formation of gas bubbles on the surface of the colony was accepted as a positive indication of catalase activity.[45] Pullulanase activity was assessed by streaking isolates onto sterile pullulan media. After incubation, the presence of clear zones around the colonies showed positive pullulanase activity.[45] Lipase activity was determined by streaking isolates onto sterile Tween 80 Agar media. After incubation period, the presence of opaque zones around the colonies indicated positive lipase activity.[45] Amylase activity was assessed by streaking haloversatile isolates onto sterile Starch media. After incubation, the entire media was covered with Gram's iodine solution. The presence of clear zones around the colonies was accepted as a positive indication of starch hydrolysis by amylase enzyme.[45] All test media were incubated at 35°C for 24 hours.

Utilization of Different Amino Acids and Carbon Sources by Haloversatile Bacteria

In this study, metabolic activities of haloversatile bacterial isolates were evaluated using five amino acids and five sugars. The utilization of amino acid sources, including 1% glycine, L-histidine, L-cysteine, L-proline, and L-threonine was examined. The medium for amino acids contained 0.05% dextrose, 0.5% beef extract, 0.0005% pyridoxal, 0.001% bromocresol purple, 0.5% peptone, and 0.0005% cresol red in 1.17% NaCl solution. Test tubes were incubated at 35°C for 24 hours after bacterial inoculation. A positive result was indicated by a change in color to purple in the test tubes.[31] The utilization and acid production from different sugar sources by the haloversatile isolates were separately tested in the test medium containing 1% lactose, galactose, maltose, xylose, and glucose. The sugar medium contained 0.001% phenol red and 0.5% yeast extract. A change in color from red to yellow was considered a positive result.[11]

Examination of the Damage Caused by Enzyme-Producing Haloversatile Bacteria on the Goatskin Sample Using Scanning Electron Microscope

Seventeen different haloversatile bacterial species (*Solibacillus silvestris*, *Bacillus licheniformis, Staphylococcus warneri*, *Bacillus sonorensis*, *Kocuria rosea*, *Oceanobacillus polygoni*, *Bacillus pumilus*, *Virgibacillus proomii*, *Staphylococcus hominis* subsp. *hominis*, *Bhargavaea ginsengi*, *Bacillus amyloliquefaciens*, *Bacillus cereus*, *Bacillus paralicheniformis*, *Alkalihalobacillus clausii*, *Staphylococcus nepalensis*, *Micrococcus luteus*, *Ornithinibacillus scapharcae*) were used as test isolates in this experiment. Firstly, fresh goatskin samples were cut into two pieces and washed with sterile distilled water three times. As a control group (first piece of fresh goat skin), 10 g of fresh goatskin sample was placed into 30 mL of sterile saline solution (15% NaCl) in an Erlenmeyer flask. To prepare the mixed bacterial culture, the turbidity of each test isolate was adjusted to McFarland 0.5 turbidity standard tube (10^8 CFU/mL). Each bacterial solution was diluted one-tenth (10^7 CFU/mL) using a sterile 1.17% NaCl solution. Then, 1.7 mL of each test isolate (17 different isolate) was mixed to prepare the the mixed haloversatile bacterial culture. The second piece of fresh goatskin (10 g) was treated with the mixed culture of test isolates (10^7 CFU/mL) in an Erlenmeyer flask. The goatskin samples were shaken for 15 hours at 45 rpm, 24°C. After that, the samples were stored for 40 days to examine the adverse effects of bacterial enzymes on the skin structure. Furthermore, organoleptic characteristics such as unacceptable odor, sticky appearance, and hair loss were investigated on the goatskin samples during the storage period. After the storage period, the goatskin samples were prepared for examination under the scanning electron microscope. Raw goatskin samples, measuring 5 mm × 5 mm, were excised using a scalpel. The skins were thoroughly cleared of any impurities and hairs. First, the skin samples were fixed in glutaraldehyde solution (4%) prepared with phosphate buffer (pH 7.2, 0.1M) for 30 min, and then the samples were washed three times in phosphate buffer (0.1M) for ten minutes. The osmium tetroxide solution (1%) prepared with phosphate buffer (0.1M) was poured on the samples at 24°C for one hour. Afterward, the skin samples were washed twice with sterile distilled water, 35%, 50%, 75%, 95%, and absolute ethanol. The skin samples were respectively treated with the mix solution of ethanol-hexamethyldisilazane (HMDS) [1:1 (v/v)] (1x30 min), ethanol-HMDS [1:2 (v/v)] (1x30 min), and HMDS (2x30 min) for the air-drying process. After air-drying process, the goatskin samples were placed in a desiccator for 14 hours for removing HMDS. The dried samples were placed on the stubs of the electron microscope using double-sided adhesive tape and examined under an electron microscope (Thermo Fisher Scientific Quattro S, Bogazici University, Istanbul, Türkiye).[54]

Destruction of Haloversatile Bacteria Using Electric Current

The mixed culture of 17 haloversatile bacterial species (*Solibacillus silvestris*, *Bacillus licheniformis, Staphylococcus warneri*, *Bacillus sonorensis*, *Kocuria rosea*, *Oceanobacillus polygoni*, *Bacillus pumilus*, *Virgibacillus proomii*, *Staphylococcus hominis* subsp. *hominis*, *Bhargavaea ginsengi*, *Bacillus amyloliquefaciens*, *Bacillus cereus*, *Bacillus paralicheniformis*, *Alkalihalobacillus clausii*, *Staphylococcus nepalensis*, *Micrococcus luteus*, *Ornithinibacillus scapharcae*) were used for the direct electric current treatment. First, the isolates were separately inoculated into test tubes containing a Halophilic Growth Medium. The test tubes were incubated at 35°C overnight. The density of each bacterial solution was adjusted to 10^7 CFU/mL using sterile saline solution (1.17% NaCl). Then, 20 mL of mixed culture was prepared by combining equal volumes from each of the 17 bacterial solutions. Subsequently, 20 mL of the mixed bacterial culture was added into a glass beaker containing 180 mL of 15% NaCl solution. Platinum wire electrodes were placed inside the glass beaker and 2.2 A direct electric current was applied to the test medium for 25 minutes. Throughout the experiment, 100 µL samples were taken from the test medium at 1, 4, 7, 10, 13, 16, 19, 22, and 25-minute intervals. These samples were then diluted and uniformly spreaded over the Halophilic Agar Medium (HAM) surface to determine the count of viable cells in the mixed culture. Colonies grown on HAM were counted after incubation at 35°C for 24 hours. At the beginning of the experiment, the pH of the test medium was 7.2, and the temperature was 22°C. The pH and temperature were measured at 1, 4, 7, 10, 13, 16, 19, 22, and 25-minute intervals during the experiment.[11,33,36,43]

Examination of Haloversatile Bacterial Cells Before and After Treatment with Direct Electric Current Using Scanning Electron Microscopy

The mixed culture of haloversatile bacterial cells was centrifuged at 10,000 rpm for 5 minutes. Subsequently, after discarding the supernatant, the bacterial cells in the pellets were washed with 0.2 M Na-phosphate-buffered saline (PBS) prepared with 20.44 g Na_2HPO_4, 6.72 g NaH_2PO_4, and 500 mL dH_2O. The bacterial cells were fixed with 0.25% glutaraldehyde and incubated at 25°C for 30 minutes, followed by 37°C for 24 hours. The bacterial cells were washed three times with Na-PBS (pH 7.2) and centrifuged to collect the pellet. After that, the pellet was subjected to a series of ethanol washes and incubated in absolute ethanol at room temperature. Then, 10 µL of the pellet was spread on a sterile slide coated with gold using a gold-coating machine at the Department of Biomedical Engineering, Marmara University.[55,56] Finally, the gold-coated samples were examined by Thermo Fisher Scientific-Quattro SEM at Bogazici University, Istanbul, Türkiye.

Results and Discussion

In the present study, we examined ten salted goatskin samples obtained from the Tuzla Leather Organized Industrial Zone. The pH values of the salted goatskin samples were found as 6.50-6.88. We determined that ten salted goatskin samples contained haloversatile bacteria on Halophilic Agar Medium between 7×10^4 and 2.7×10^5 CFU/g (Table I). The total proteolytic haloversatile bacterial counts on salted goatskin samples were found as between 1×10^4 and 8×10^4 CFU/g on Gelatin Agar Medium and the total lipolytic haloversatile bacterial counts on salted goatskin samples were found as between 1×10^4 and 1.3×10^5 CFU/g on Tween 80 Agar Medium (Table I). In a previous study conducted by Ozbay and Caglayan (2022)[22] on haloversatile bacteria, the total counts of haloversatile bacteria in the soaking liquids collected from tanneries were found to be in the range of 3.8×10^4 to 1.1×10^6 CFU/mL on Oligotrophic Agar Medium and 6.7×10^4 to 1.6×10^6 CFU/mL on Halophilic Agar Medium. In that study, the researchers also reported that the total proteolytic haloversatile bacterial counts in the samples were found to be in the range of 1.2×10^4 to 5.8×10^5 CFU/mL on Gelatin Agar Medium.[22] Additionally, the total lipolytic haloversatile bacterial counts were determined to be in the range of 2.3×10^4 to 4.6×10^5 CFU/mL on Tween 80 Agar Medium and 6.0×10^3 to 1.5×10^5 CFU/mL on Rhodamine B-Olive Oil Agar Medium.[22] In the present study, haloversatile, proteolytic haloversatile and lipolytic haloversatile bacteria were found on all salted goatskin samples. The pH values of the salted goatskin samples were found as 6.50-6.88 (Table I).

A total of 26 isolates were obtained from salted goat skin samples. These isolates were identified as *Staphylococcus warneri*, *Alkalihalobacillus clausii*, *Solibacillus silvestris*, *Bacillus licheniformis*, *Bacillus pumilus*, *Ornithinibacillus scapharcae*, *Kocuria rosea*, *Oceanobacillus polygoni*, *Virgibacillus proomii*, *Staphylococcus hominis* subsp. *hominis*, *Bhargavaea ginsengi*, *Bacillus amyloliquefaciens*, *Bacillus licheniformis*, *Bacillus cereus*, *Bacillus paralicheniformis*, *Staphylococcus nepalensis*, and *Micrococcus luteus*. While four, three, and two strains of *Staphylococcus warneri*, *Alkalihalobacillus clausii*, and *Solibacillus silvestris* were respectively isolated from the salted goat skin samples, only one strain of the other bacterial species was recovered from the salted goat skin samples (Table II).

In previous study, Caglayan (2019)[31] isolated different haloversatile species such as *Exiguobacterium sibiricum*, *Bacillus subtilis* subsp.*stercoris*, *Bacillus haynesii*, *Paracoccus marcusii*, *Kocuria polaris*, *Acinetobacter radioresistens*, *Micrococcus aloeverae*, *Bacillus pumilus*, *Microbacterium maritypicum*, *Microbacterium aurantiacum*, *Brevibacterium frigoritolerans*, *Staphylococcus lentus*, *Paracoccus hibiscisoli*, *Staphylococcus hominis* subsp. *novobiosepticus*, *Bacillus velezensis*, *Staphylococcus equorum* subsp. *equorum*, *Bacillus safensis*, *Kocuria sediminis*, *Staphylococcus petrasii* subsp.*jettensis*, *Staphylococcus pasteuri*, *Bacillus thioparans*, *Staphylococcus warneri*, *Virgibacillus salarius*, *Bacillus paraflexus*, *Pseudomonas songnenensis*, *Microbacterium saccharophilum*, *Bacillus altitudinis*, *Staphylococcus saprophyticus* subsp.*saprophyticus*, *Gordonia alkanivorans*, *Micrococcus yunnanensis*, *Agrococcus lahaulensis*, *Kocuria rosea*, *Sanguibacter inulinus*, *Bacillus nealsonii*, *Staphylococcus cohnii* subsp. *urealyticus*, *Bacillus oryzaecorticis*, *Exiguobacterium artemiae*, *Exiguobacterium indicum*, *Bacillus siamensis*, and *Staphylococcus epidermidis* from 20 salt samples collected from Camalti Saltern. Caglayan (2022)[31] also isolated and identified 16 haloversatile bacteria

Table I

The Salted Skin Sample Codes, pH of Salted Skin Samples, Total Haloversatile, Total Proteolytic Haloversatile, Total Lipolytic Haloversatile Bacterial Counts on Salted Goatskin Samples (CFU/g)

Sample no	Skin sample code	pH of skin	Total counts of haloversatile bacteria (CFU/g)	Total counts of proteolytic haloversatile bacteria (CFU/g)	Total counts of lipolytic haloversatile bacteria (CFU/g)
1	SSS1	6.79	1.3×10^5	1×10^4	1×10^4
2	SSS2	6.64	8×10^4	3×10^4	2×10^4
3	SSS3	6.76	1.5×10^5	5×10^4	1.3×10^5
4	SSS4	6.68	1.6×10^5	4×10^4	6×10^4
5	SSS5	6.68	8×10^4	2×10^4	1×10^4
6	SSS6	6.86	1×10^5	8×10^4	8×10^4
7	SSS7	6.88	2.7×10^5	5×10^4	2×10^4
8	SSS8	6.75	9×10^4	1×10^4	6×10^4
9	SSS9	6.61	1.5×10^5	3×10^4	4×10^4
10	SSS10	6.50	7×10^4	1×10^4	3×10^4

SGS: Salted Goatskin Sample

Table II

The Isolate Codes, Phylogenetically Similar Species, Length (bp), Similarity (%), Accession Number of Haloversatile Isolates obtained from Salted Goatskin Samples

	Isolate code	Phylogenetically similar species	Length (bp)	Similarity (%)	Accession Number
1	S1a	*Solibacillus silvestris*	1371	99.40	MT013412
2	S1b	*Bacillus licheniformis*	1451	99.24	MN368292
3	S2a	*Staphylococcus warneri*	1495	100	MT642942
4	S2b	*Bacillus sonorensis*	1451	99.50	MN710423
5	S2c	*Kocuria rosea*	1457	99.37	MT225716
6	S3a	*Oceanobacillus polygoni*	1518	99.65	NR114348
7	S3b	*Bacillus pumilus*	1263	99.74	KR006242
8	S3c	*Virgibacillus proomii*	1405	99.80	KT893316
9	S4a	*Staphylococcus hominis* subsp. *hominis*	1463	99.55	MT585539
10	S4b	*Bhargavaea ginsengi*	1506	99.56	MN121192
11	S4c	*Bacillus amyloliquefaciens*	1498	99.45	MT133342
12	S4d	*Bacillus licheniformis*	1145	99.81	MT492090
13	S5a	*Bacillus cereus*	1297	99.90	HE660038
14	S5b	*Bacillus paralicheniformis*	1178	99.73	OP700359
15	S6a	*Alkalihalobacillus clausii*	1407	99.70	MH938303
16	S6b	*Solibacillus silvestris*	1371	99.77	MT013412
17	S6c	*Staphylococcus nepalensis*	1340	99.91	LC511694
18	S7a	*Staphylococcus warneri*	1276	99.62	MK491025
19	S7b	*Staphylococcus warneri*	1495	99.70	MT642942
20	S8a	*Micrococcus luteus*	1455	99.47	MH669309
21	S8b	*Ornithinibacillus scapharcae*	1434	99.63	MK860001
22	S8c	*Alkalihalobacillus clausii*	1370	99.81	MT604989
23	S9a	*Staphylococcus warneri*	1495	99.61	MT642942
24	S10a	*Ornithinibacillus scapharcae*	1434	99.03	MK860001
25	S10b	*Alkalihalobacillus clausii*	1407	99.70	MH938303
26	S10c	*Bacillus pumilus*	1094	99.32	MK377090

which were obtained from brine samples of Camalti Saltern. Those isolates belong to the species *Rhodococcus enclensis*, *Bacillus haynesii*, *Kocuria sediminis*, *Bacillus simplex*, *Salinivibrio costicola* subsp. *vallismortis*, *Bacillus subtilis* subsp. *stercoris*, *Vibrio olivae*, *Bacillus pumilus*, *Staphylococcus saprophyticus* subsp. *saprophyticus*, *Staphylococcus petrasii* subsp. *jettensis*, *Marinomonas communis*, *Marinobacter hydrocarbonoclasticus*, *Vibrio neocaledonicus*, and *Pseudomonas psychrotolerans*.[32] Ozbay and Caglayan (2022)[22] reported that six haloversatile bacterial isolates were obtained from soak liquor samples collected from leather industry and identified as *Bacillus mojavensis*, *Bacillus australimaris*, *Brevibacterium luteolum*, *Bacillus siamensis*, and *Terribacillus halophilus*. Haloversatile *Staphylococcus*, *Bacillus*, and *Kocuria* species were also isolated by other researchers[22,31,32] but the isolation of haloversatile *Oceanobacillus polygoni*, *Virgibacillus proomii*, *Bhargavaea ginsengi*, *Ornithinibacillus scapharcae*, and *Alkalihalobacillus clausii* from the salted goat skin samples have first been reported in the present study.

All isolates were Gram-positive and grew optimally at pH 7, 1.17% NaCl, 35°C (Table III). Also, *Bacillus paralicheniformis* isolate S5b grew optimally at pH 8 (Table III). Isolates S1a, S2a, S4b, S4c, S4d, S5a, S5b S6b, S6c, S7a, S7b, S9a, S10c; isolates S1b, S2b, S3a, S3b, S6a, SS8c, S10b; isolates S2c, S3c, S8a, S8b, S10a were respectively showed growth at pH 5-11, pH 5-12, pH 6-11 (Table

Table III

The Effects of pH, NaCl Contents and Temperature Values on the Growth of Haloversatile Bacterial Isolates

	Isolate code	Isolate name	Optimum pH	Range of pH	Optimum NaCl (%)	Range of NaCl (%)	Optimum temperature(°C)	Range of temperature (°C)	Gram Stain
1	S1a	*Solibacillus silvestris*	7	5-11	1.17	0-17.5	35	20-50	+
2	S1b	*Bacillus licheniformis*	7	5-12	1.17	0-17.5	35	15-55	+
3	S2a	*Staphylococcus warneri*	7	5-11	1.17	0-17.5	35	20-50	+
4	S2b	*Bacillus sonorensis*	7	5-12	1.17	0-17.5	35	15-55	+
5	S2c	*Kocuria rosea*	7	6-11	1.17	0-17.5	35	20-45	+
6	S3a	*Oceanobacillus polygoni*	7	5-12	1.17	0-17.5	35	15-55	+
7	S3b	*Bacillus pumilus*	7	5-12	1.17	0-17.5	35	15-55	+
8	S3c	*Virgibacillus proomii*	7	6-11	1.17	0-17.5	35	20-50	+
9	S4a	*Staphylococcus hominis* subsp. *hominis*	7	6-12	1.17	0-17.5	35	20-45	+
10	S4b	*Bhargavaea ginsengi*	7	5-11	1.17	0-17.5	35	20-45	+
11	S4c	*Bacillus amyloliquefaciens*	7	5-11	1.17	0-17.5	35	15-55	+
12	S4d	*Bacillus licheniformis*	7	5-11	1.17	0-17.5	35	15-55	+
13	S5a	*Bacillus cereus*	7	5-11	1.17	0-17.5	35	15-55	+
14	S5b	*Bacillus paralicheniformis*	7-8	5-11	1.17	0-17.5	35-37	15-55	+
15	S6a	*Alkalihalobacillus clausii*	7	5-12	1.17	0-17.5	35	20-45	+
16	S6b	*Solibacillus silvestris*	7	5-11	1.17	0-17.5	35	20-45	+
17	S6c	*Staphylococcus nepalensis*	7	5-11	1.17	0-17.5	35	20-45	+
18	S7a	*Staphylococcus warneri*	7	5-11	1.17	0-17.5	35	20-50	+
19	S7b	*Staphylococcus warneri*	7	5-11	1.17	0-17.5	35	20-50	+
20	S8a	*Micrococcus luteus*	7	6-11	1.17	0-17.5	35	20-45	+
21	S8b	*Ornithinibacillus scapharcae*	7	6-11	1.17	0-17.5	35	20-45	+
22	S8c	*Alkalihalobacillus clausii*	7	5-12	1.17	0-17.5	35	20-45	+
23	S9a	*Staphylococcus warneri*	7	5-11	1.17	0-17.5	35	20-50	+
24	S10a	*Ornithinibacillus scapharcae*	7	6-11	1.17	0-17.5	35	20-50	+
25	S10b	*Alkalihalobacillus clausii*	7	5-12	1.17	0-17.5	35	20-45	+
26	S10c	*Bacillus pumilus*	7	5-11	1.17	0-17.5	35	15-55	+

III). Although all isolates were able to grow at 0-17.5% NaCl, the optimum growth value was 1.17% NaCl. Hence, all isolates were accepted as haloversatile.[25,26] The growth temperature values of the isolates were slightly different from each other. Isolates S1b, S2b, S3a, S3b,S4c, S4d, S5a, S5b, S10c; isolates S1a, S2a, S3c, S7a, S7b, S9a, S10a; isolates S2c, S4a, S4b, S6a, S6b, S6c, S8a, S8b, S8c, S10b were respectively exhibited growth at 15-55°C**,** 20-50°C, 20-45°C (Table III).

Staphylococcus saprophyticus subsp.*saprophyticus*, *Bacillus simplex*, *Bacillus pumilus*, *Marinobacter hydrocarbonoclasticus*, *Staphylococcus petrasii* subsp.*jettensis*, *Vibrio neocaledonicus*, *Salinivibrio costicola* subsp.*vallismortis*, *Bacillus haynesii*, *Kocuria sediminis*, *Pseudomonas psychrotolerans*, *Rhodococcus enclensis*, *Marinomonas communis*, *Vibrio olivae*, *Bacillus subtilis* subsp.*stercoris* which were previously isolated from the brine samples of Camalti Saltern were able to grow at 0-3 M NaCl (optimum growth at 0.2 M NaCl), pH 5-12 and 10-55°C.[32]

When we examined the enzymatic activities of 26 haloversatile bacteria isolated from salted goatskin samples, they exhibited enzymatic activities as follows: 88% protease-positive, 69% lipase-

Table IV

Enzymatic Characteristics of Haloversatile Isolates obtained from Salted Goatskin Samples

	Isolate code	Haloversatile species	Protease	Lipase	Xylanase	Pullulanase	Caseinase	Amylase	DNase	Cellulase	Urease	Catalase	Oxidase
1	S1a	*Solibacillus silvestris*	+	–	–	–	–	–	–	–	+	+	–
2	S1b	*Bacillus licheniformis*	+	+	–	–	+	+	–	+	–	+	+
3	S2a	*Staphylococcus warneri*	+	+	–	–	–	–	–	–	+	+	–
4	S2b	*Bacillus sonorensis*	+	+	–	–	–	+	–	+	–	+	+
5	S2c	*Kocuria rosea*	+	–	–	–	–	–	–	–	–	+	+
6	S3a	*Oceanobacillus polygoni*	–	–	–	–	–	–	–	–	+	+	+
7	S3b	*Bacillus pumilus*	+	+	–	–	+	–	–	+	+	+	+
8	S3c	*Virgibacillus proomii*	+	+	–	–	–	–	+	–	+	+	–
9	S4a	*Staphylococcus hominis* subsp. *hominis*	–	–	–	–	–	–	–	–	–	+	–
10	S4b	*Bhargavaea ginsengi*	+	–	–	–	–	–	+	–	–	+	–
11	S4c	*Bacillus amyloliquefaciens*	+	–	–	–	–	+	–	+	–	+	+
12	S4d	*Bacillus licheniformis*	+	+	–	–	+	+	–	+	–	+	+
13	S5a	*Bacillus cereus*	+	+	–	–	+	+	–	–	–	+	–
14	S5b	*Bacillus paralicheniformis*	+	+	–	–	–	+	–	–	–	+	–
15	S6a	*Alkalihalobacillus clausii*	+	+	–	–	–	–	–	–	+	+	+
16	S6b	*Solibacillus silvestris*	+	–	–	–	–	–	–	–	+	+	–
17	S6c	*Staphylococcus nepalensis*	–	+	–	–	–	–	–	–	+	+	–
18	S7a	*Staphylococcus warneri*	+	+	–	–	–	–	–	–	+	+	–
19	S7b	*Staphylococcus warneri*	+	+	–	–	–	–	–	–	+	+	–
20	S8a	*Micrococcus luteus*	+	–	–	–	–	–	–	–	–	+	+
21	S8b	*Ornithinibacillus scapharcae*	+	+	+	–	+	–	–	+	–	+	+
22	S8c	*Alkalihalobacillus clausii*	+	+	–	–	–	–	–	–	+	+	+
23	S9a	*Staphylococcus warneri*	+	+	–	–	–	–	–	–	+	+	–
24	S10a	*Ornithinibacillus scapharcae*	+	+	+	–	+	–	–	+	–	+	+
25	S10b	*Alkalihalobacillus clausii*	+	+	–	–	–	–	–	–	+	+	+
26	S10c	*Bacillus pumilus*	+	+	–	–	+	–	–	+	+	+	+

positive, 8% xylanase-positive, 27% caseinase-positive, 23% amylase-positive, 8% DNase-positive, 31% cellulase-positive, 54% urease-positive, 100% catalase-positive, 54% oxidase-positive, and 100% pullulanase-negative (Table IV).

Haloversatile isolates reported by Ozbay and Caglayan (2022)[22] were able to produce protease (83%), lipase (83%), caseinase (67%), amylase (50%), cellulase (17%). However, those isolates did not produce xylanase, DNase, pullulanase and urease.[22]

Table V shows the utilization of different sugars (lactose, galactose, xylose, glucose, maltose) and different amino acids (L-cysteine, L-proline, L-threonine, L-histidine, glycine) by haloversatile bacterial isolates. The bacterial isolates showed positive results for lactose at 42%. For galactose, the isolates showed a positive result of 46%. For xylose, the positivity rate was 58%. As for glucose, 81% of the isolates gave a positive result, while maltose resulted in 73% positivity (Table V). These results provide insights into how microorganisms metabolize different sugars. It was concluded that

Table V

Utilization of Different Sugars and Amino Acids by Haloversatile Isolates

	Isolate code	Haloversatile species	Lactose	Galactose	Xylose	Glucose	Maltose	L-cysteine	L-proline	L-threonine	L-histidine	Glycine
1	S1a	*Solibacillus silvestris*	–	–	–	–	–	–	+	+	–	+
2	S1b	*Bacillus licheniformis*	+	–	+	+	+	–	–	+	–	+
3	S2a	*Staphylococcus warneri*	–	–	–	+	+	+	+	+	+	+
4	S2b	*Bacillus sonorensis*	–	+	+	+	+	+	–	–	–	–
5	S2c	*Kocuria rosea*	–	–	+	+	–	+	+	+	+	+
6	S3a	*Oceanobacillus polygoni*	–	–	–	–	+	+	+	–	–	+
7	S3b	*Bacillus pumilus*	+	+	+	+	–	+	+	+	–	+
8	S3c	*Virgibacillus proomii*	–	+	–	+	+	+	+	+	+	+
9	S4a	*Staphylococcus hominis* subsp. *hominis*	+	+	–	+	+	+	+	+	–	+
10	S4b	*Bhargavaea ginsengi*	–	–	+	+	+	+	+	+	+	+
11	S4c	*Bacillus amyloliquefaciens*	+	+	+	+	+	+	+	+	–	–
12	S4d	*Bacillus licheniformis*	+	–	+	+	+	–	–	+	–	+
13	S5a	*Bacillus cereus*	–	–	–	+	+	+	+	–	+	+
14	S5b	*Bacillus paralicheniformis*	+	–	+	+	+	+	–	+	–	–
15	S6a	*Alkalihalobacillus clausii*	+	+	+	+	+	+	+	–	–	+
16	S6b	*Solibacillus silvestris*	–	–	–	–	–	–	+	+	–	+
17	S6c	*Staphylococcus nepalensis*	+	+	+	+	+	–	–	+	–	+
18	S7a	*Staphylococcus warneri*	–	–	–	+	+	+	+	+	+	+
19	S7b	*Staphylococcus warneri*	–	–	–	+	+	+	+	+	+	+
20	S8a	*Micrococcus luteus*	–	–	–	+	+	+	+	+	–	+
21	S8b	*Ornithinibacillus scapharcae*	–	+	+	–	–	+	+	+	–	+
22	S8c	*Alkalihalobacillus clausii*	+	+	+	+	+	+	+	–	–	+
23	S9a	*Staphylococcus warneri*	–	–	–	+	+	+	+	+	+	+
24	S10a	*Ornithinibacillus scapharcae*	–	+	+	–	–	+	+	+	–	+
25	S10b	*Alkalihalobacillus clausii*	+	+	+	+	+	+	+	–	–	+
26	S10c	*Bacillus pumilus*	+	+	+	+	–	+	+	+	–	+

the haloversatile bacteria in the skin primarily utilize glucose and have the least utilization of lactose.

It has been known that collagen types I and III contain alanine, arginine, asparagine, aspartic acid, glutamic acid, glutamine, glycine, histidine, hydroxylysine, hydroxyproline, isoleucine, leucine, lysine, methionine, phenylalanine, proline, serine, threonine, tyrosine and valine.[57] While alanine, arginine, asparagine, aspartic acid, cysteine, glutamic acid, glutamine, glycine, hydroxyproline, isoleucine, leucine, lysine, phenylalanine, proline, serine, threonine, tyrosine, and valine[57] are found in elastin, keratin contains alanine, arginine, asparagine, aspartic acid, cysteine, glutamic acid, glutamine, glycine, histidine, isoleucine, leucine, lysine, methionine, phenylalanine, proline, serine, threonine, tyrosine, tryptophan, and valine.[57]

The bacterial isolates showed positive results for L-cysteine at 80%. For L-proline, the isolates yielded an 80% positive result. L-threonine resulted in 80% positivity as well. However, only 31% of the isolates showed a positive result for L-histidine. As for glycine, 88% of the isolates demonstrated a positive result (Table V). These results provide insights into how microorganisms metabolize

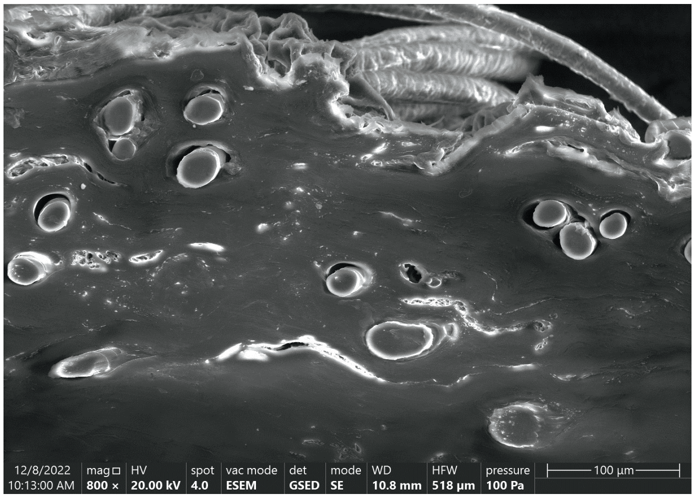

Figure 1. SEM micrograph of the longitudinal section of undamaged goatskin treated with sterile brine solution stored for 40 days at 24°C (Control). The bar: 100 µm.

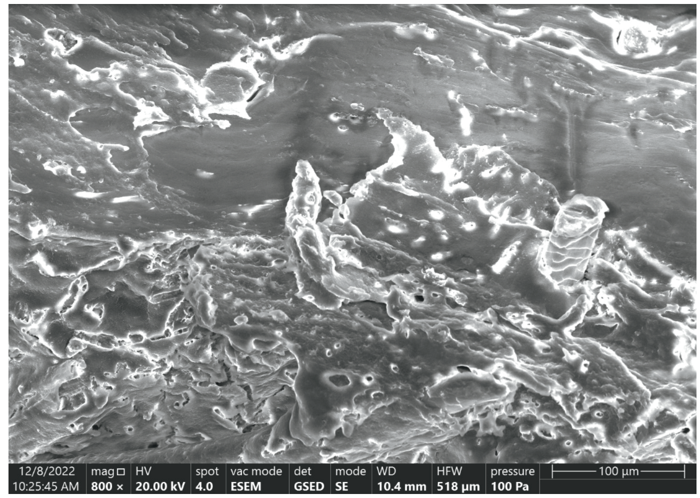

Figure 2. SEM micrograph of the longitudinal section of damaged goatskin treated with mixed culture of haloversatile isolates stored for 40 days at 24°C. The bar: 100 µm.

different amino acids. It was determined that the haloversatile bacteria in the skin primarily utilize glycine and have the least utilization of L-histidine. These results showed that proteolytic haloversatile strains have the potential utilization of amino acids as nitrogen sources to grow on the skin after the breakdown of protein into amino acids.

Different sugar sources such as lactose (100%), dextrose (100%), myo-inositol (100%), cellobiose (100%), adonitol (100%), salicin (100%), dulcitol (100%), mannose (100%), xylitol (83%), arabinose (83%), mannitol (67%), fructose (67%), trehalose (67%), ribose (50%), melezitose (33%), sucrose (17%) and different amino acid sources such as L-serine (100%), L-glutamic acid (67%), L-phenylalanine (67%), trans-4-hydroxy-L-proline (67%), L-proline (67%), glycine (50%), L-ornithine (50%), L-aspartic acid (33%), L-phenylalanine (33%), L-arginine (17%), L-histidine (17%), L-lysine (17%), L-threonine (17%) were used by haloversatile bacteria isolated from the soak liquors.[22] However, sorbitol, galactose, maltose, xylose and melibiose, L-isoleucine, L-cystine, L-alanine, leucine, L-methionine, L-tyrosine, L-valine were not utilized by the isolates.[22]

At the end of the 40-days storage period, the changes on the structure of the goatskin control sample (Figure 1) and the goatskin sample treated with the mixed culture of 17 different haloversatile bacterial species (Figure 2) caused by the haloversatile bacteria were investigated under scanning electron microscope. On the goatskin control sample, it was clearly observed that there was no hair loss, and the skin integrity was preserved (Figure 1).

TABLE VI

The pH values, temperature, voltage and the total counts (CFU/mL) of enzyme producing haloversatile bacteria in the direct electric current treatment

Time	pH value	Temperature (°C)	Voltage (V)	Total counts of mixed culture (CFU/mL)
Before experiment	7.2	22	6.5	7.3×10^6
1 min	7.2	22	6.5	1.4×10^5
4 min	7.3	22	6.4	2.5×10^4
7 min	7.3	23	6.2	5.4×10^3
10 min	7.4	24	5.9	1.6×10^2
13 min	7.4	25	5.7	8×10^1
16 min	7.5	26	5.5	4
19 min	7.5	27	5.3	-
22 min	7.6	28	5.1	-
25 min	7.6	29	4.9	-

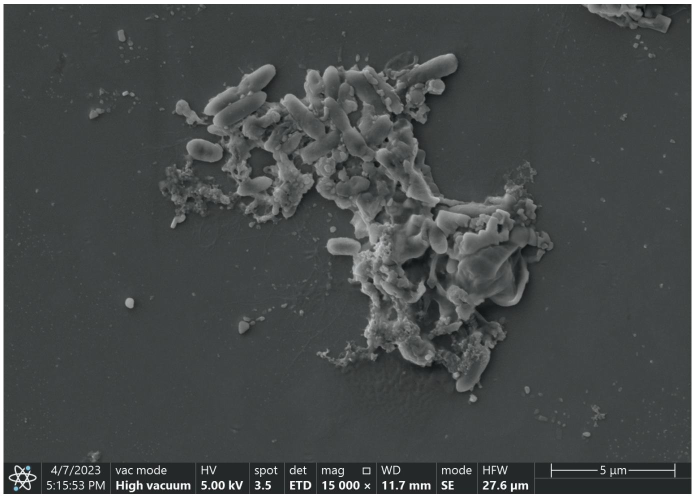

Figure 3. SEM micrograph of the mixed culture of enzyme producing haloversatile bacterial cells before direct electric current treatment. The bar: 5 µm.

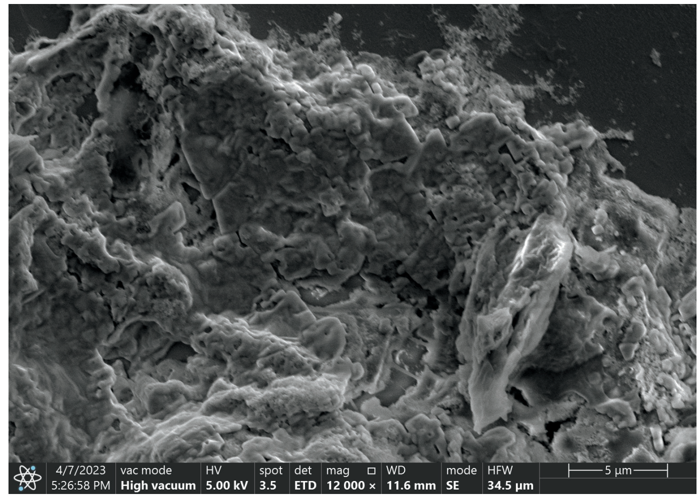

Figure 4. SEM micrograph of damaged bacterial cells in the mixed culture after direct electric current treatment. The bar: 5 µm.

Softening and decomposition were observed on the goatskin sample treated with the mixed culture of test bacteria (Figure 2). In addition, environmental scanning electron microscope image clearly showed that the hair follicles in the goatskin were damaged, hairs were broken, and the fibrous structure of the skin was disrupted (Figure 2).

Figure 2 shows the damage caused by the mixed culture of enzyme-producing haloversatile bacteria to the structure of goatskin. Hair loss can be observed in the goatskin (Figure 2). Scanning electron micrograph demonstrates that the haloversatile isolates in the mixed culture destroy the collagen fibers and hairs of the skin.

Before the electric current treatment, the total viable cell count of the mixed culture was 7.3×10^6 CFU/mL (Table VI). During the electric current treatment, the mixed haloversatile bacterial cells were gradually killed. After 16 minutes, it decreased to 4 CFU/mL. After 19 minutes, all test bacteria in the mixed culture were completely killed. While the pH was 7.2 before the experiment, the pH was reached to 7.6 at the end of the experiment. The temperature increased from 22°C to 29°C (Table VI). The voltage values were slightly decreased from 6.5 to 4.9 (Table VI).

Figure 3 clearly shows the morphological structures of enzyme-producing haloversatile bacterial cells in the mixed culture before the direct electric current treatment in the SEM micrograph.

Figure 4 shows the damaged cell structure of enzyme-producing haloversatile bacteria in the mixed culture after direct electric current treatment in the SEM micrograph.

In a study conducted by Birbir and colleagues in 2008, inactivation of extremely halophilic bacteria in salt samples was achieved with a direct electric current of 0.5 A.[34,35] In another study, 1.5 A alternating electric current was used to eliminate a mixed culture of *Enterobacter cloacae*, *Pseudomonas luteola*, and *Vibrio fluvialis*, which were Gram-negative bacteria isolated from hides. The mixed culture of bacteria in the liquid medium containing 25% NaCl was eradicated within 1 minute using a 1.5 A alternating electric current.[58]

The negative effects of protease and lipase positive extremely halophilic archaea against sheepskin structure were previously reported by Birbir and her colleagues in 2020.[9] In a different research, the detrimental impacts of Gram-positive haloversatile bacteria isolated from soak liquor samples on the skin samples were proven.[22] The results obtained from other studies were also similar to the results of this study. The haloversatile bacteria are able to survive under harsh conditions and damage goatskin structure. However, the application of electric current was found to be very effective in killing different species of haloversatile bacteria. In just 19 minutes, all 17 haloversatile bacteria in the mixed culture were successfully eliminated. This impressive outcome demonstrates the effectiveness of the electric current inactivation method and highlights its potential for use in the leather industry.

Conclusion

This study is the first to contribute to the characterization of haloversatile bacteria found in salted goatskin samples, the investigation of the harmful effects of enzyme-producing haloversatile bacteria on the skin under environmental scanning electron microscopy, and the application of direct electric current to kill bacteria in a mixed culture of enzyme-producing haloversatile isolates. We detected that haloversatile bacteria produced different enzymes and utilized different amino acid and sugar sources. Based on the results of 16S rRNA sequencing, the 26 isolated haloversatile bacterial isolates were found to belong to 17 different species, including *Solibacillus silvestris*, *Bacillus licheniformis*, *Staphylococcus warneri*, *Bacillus sonorensis*, *Kocuria rosea*, *Oceanobacillus polygoni*, *Bacillus pumilus*, *Virgibacillus proomii*, *Staphylococcus hominis* subsp. *hominis*, *Bhargavaea ginsengi*, *Bacillus amyloliquefaciens*, *Bacillus cereus*, *Bacillus paralicheniformis*, *Alkalihalobacillus clausii*, *Staphylococcus nepalensis*, *Micrococcus luteus*, *Ornithinibacillus scapharcae*. According to our experimental results, we have found that the application of direct electric current can easily kill haloversatile bacterial species belonging to Gram-positive genera, including *Solibacillus*, *Staphylococcus*, *Kocuria*, *Oceanobacillus*, *Virgibacillus*, *Bhargavaea*, *Alkalihalobacillus*, *Micrococcus*, *Ornithinibacillus*, and *Bacillus*. This result suggests that this method can be a potential method to eliminate bacteria. This technique can be used in the leather industry, providing a simple, safe, broad-spectrum antibacterial activity and cost-effective solution. Therefore, we plan to conduct more detailed research in our further experiments to explore its effective use in brine curing of hides and skins.

Acknowledgements

This study was supported by the Scientific Research Project Commission of Marmara University, Project No FYL-2022-10598. We would like to thank the Scientific Research Project Commission of Marmara University. We also express our gratitude to the tanneries located in the Tuzla-Istanbul Leather Organized Tannery Region in Türkiye for providing us with leather samples.

References

1. Dixit, S., Yadav, A., Dwivedi, P.D., Das, M.; Toxic Hazards of Leather Industry and Technologies to Combat Threat: A Review. *J. Clean. Prod.* **87**, 39-49, 2015.
2. Sivaram, N.M., Barik, D.; Toxic Waste From Leather Industries, Energy from Toxic Organic Waste for Heat and Power Generation, Chapter **5**, pp.55-67, 2019.
3. Kanagaraj, J., Velappan, K.C., Babu, N.K., Sadulla, S.; Solid Wastes Generation in the Leather Industry and its Utilization for Cleaner Environment. *J. Sci. Ind. Res.* **65**, 541-548, 2006.
4. Tancous, J.J.; Microorganisms in the Skin and Hide Industry. American Institute of Biological Sciences, Washington, D.C., **5**, p.21, 1964.
5. Kallenberger, W.E., Lollar, R.M.; Halophilic Bacteria Thrive in Seasonal Cycles. *J. Am. Leather Chem. Association* **81**, 248-264, 1986.
6. Akpolat, C., Ventosa, A., Birbir, M., Sánchez-Porro, C., Caglayan, P.; Molecular Identification of Moderately Halophilic Bacteria and Extremely Halophilic Archaea Isolated from Salted Sheep Skins Containing Red and Yellow Discoloratios. *JALCA***110**, 211-220, 2015.
7. Bailey, D.G., Birbir, M.; A Study of the Extremely Halophilic Microorganisms Found on Commercially Brine-cured Cattle Hides. *JALCA* **88**, 285-293, 1993.
8. Berber, D., Birbir, M.; Examination of Bacterial Populations in Salt, Salted Hides, Soaked Hides and Soak Liquors. *JALCA* **105**, 320-326, 2010.
9. Birbir, M., Caglayan, P., Birbir, Y.; The Destructive Effects of Extremely Halophilic Archaeal Strains on Sheepskins and Proposals for Remedial Curing Processes. *Johnson Matthey Technol. Rev.* **4**, 489-503, 2020.
10. Caglayan, P., Birbir, M., Sánchez-Porro, C., Ventosa, A.; Screening of Industrially Important Enzymes Produced by Moderately Halophilic Bacteria Isolated from Salted Sheep Skins of Diverse Origin. *JALCA* **112**, 207-216, 2017.
11. Caglayan, P., Birbir, M., Sánchez-Porro, C., Ventosa, A.; Detection of Industrially Potential Enzymes of Moderately Halophilic Bacteria on Salted Goat Skins. *Turk. J. Biochem.* **43**, 312-322, 2018.
12. Caglayan, P., Birbir, M., Ventosa, A., Sánchez-Porro, C.; Characterization of Moderately Halophilic Bacteria from the Salt-pack Cured Hides. *J. Soc. Leather Technol. Chem.* **5**, 250-254, 2015.
13. Sánchez-Porro, C., Yilmaz, P., De La Haba, R.R., Birbir, M., Ventosa, A.; *Thalassobacillus pellis* sp. nov., a Moderately Halophilic, Gram-positive Bacterium isolated from Salted Hides. *Int. J. Syst. Evol. Microbiol.* **5**, 1206-1210, 2011.
14. Birbir, M., Kizilkaya, K., Caglayan, P.; Examination of Moderately Halophilic Bacteria in Salt Samples Used in Hide and Skin Preservation. *J. Soc. Leather Technol. Chem.* **105**(5), 231-241, 2021.
15. Anderson, H.; The Bacteriology of the Hide Preservation. *J. Soc. Leather Technol. Chem.* **33**, 251-256, 1949.
16. Venkatesan, R.A., Nandy, S.C., Sen, S.N.; Effect of Storage and Pretanning Operations on the Bacterial Flora and its Population on Goat Skin. *Leather Science* **17**, 395-404, 1970.
17. Bailey, D.G., Birbir, M.; The Impact of Halophilic Organisms on the Grain Quality of Brine Cured Hides. *JALCA* **91**, 47-51, 1996.
18. Aslan, E., Birbir, M.; Examination of Gram-Positive Bacteria on Salt-Pack Cured Hides. *JALCA* **12**(106), 372-380, 2011.
19. Aslan, E. and Birbir, M.; Examination of Gram-Negative Bacteria on Salt-Pack Cured Hides. *JALCA* **4**(107), 106-115, 2012.
20. Bitlisli, B.O., Karavana, H.A., Basaran, B., Sarı O., Yasa, I., Birbir, M.; The Effect of Conservation Defects on the Suede Quality of Double-Face. *JALCA* **99**(12), 494-501, 2004.
21. Woods, D.R., Welton, R.L., Thomson, J.A., Cooper, D.R.; The Microbiology of Curing and Tanning Processes Part IV. Collagenolytic Activity of Bacteria from Raw and Cured Hides. *JALCA* **67**, 217-225, 1972.
22. Ozbay, O., Caglayan, P.; Identification of Gram-positive Haloversatile Bacteria in Soak Liquor Samples and Observation

of Their Damage to Sheep Skin by Scanning Electron Microscopy. *JALCA* **106**(6), 255-263, 2022.
23. Oren, A.; Life at High Salt Concentrations. The Prokaryotes 3rd Edition*;* **2**, 263-282, 2006.
24. Caviccihioli, R., Thomas, T.; Extremophiles, Schaechter, M., Lederberg, J., In: The Desk Encyclopedia of Microbiology, Chapter 37, Elsevier Academic Press., 2004.
25. Kushner, D.J.; Life in High Salt and Solute Concentrations: Halophilic Bacteria. In: Kushner, D.J., Editor. Microbial Life in Extreme Environments, London, Academic Press, pp.317-368, 1978.
26. Grant, W.D., Gemmell, R.T., Mcgenity, T.J.; *Extremophiles:* Microbiol Life in Extreme Environment. New York: Wiley-Liss Inc., 1998.
27. Ellis-Evans, J.C.; Microbial Ecology in Antarctica. *Biologist* **32**, 171-176. 1985
28. Martin, D.D., Bartlett, D.H., Roberts, M.F.; Solute Accumulation in the Deep-sea Bacterium *Photobacterium profundum*. *Extremophiles* **6**, 507-514, 2002.
29. Kaye, J.Z., Sylvan, J.B., Edwards, K.J., Baross, J.A.; *Halomonas* and *Marinobacter* Ecotypes from Hydrothermal Vent, Subseafloor and Deep-Sea Environments. *FEMS Microbiology Ecology* **75**(1), 123-133, 2011.
30. Shatla, S.H., El-Kafrawy, S.B., Ahmed, H.A., El-Mokadem, M.T.; An Integrating Geospatial Technology with Microbiology in Isolating and Characterizing Selenite-reducing Bacteria from Two Mangrove Areas along the Red Sea, Egypt. *Egypt. J. Aquat. Biol. Fish*. **25**(1), 389-405, 2021.
31. Caglayan, P.; Enzymatic Reactions and Phylogenetic Analysis of Haloversatile Bacteria isolated from Çamaltı Saltern Salt Samples used in Leather Industry. *JALCA* **115**, 450-461, 2019.
32. Caglayan, P.; Characterization and Control of Antibiotic-Resistant Camalti Saltern's Isolates with Bacteriocins. *JALCA* **117**(8), 315-329, 2022.
33. Birbir, Y., Birbir, M.; Inactivation of Extremely Halophilic Hide-Damaging Bacteria via Low-Level Direct Electric Current. *J. Electrostat*. **64**(12), 791-795, 2006.
34. Birbir, M., Ozdogru, Z. B., Birbir, Y., Ogan, A.; Extracellular Protease Activities of Extremely Halophilic Archaea and their Control via Direct Electric Current. *J. Soc. Leather Technol. Chem.* **92**(2), 53-58, 2008a.
35. Birbir, Y., Degirmenci, D., Birbir, M.; Direct Electric Current Utilization in Destruction of Extremely Halophilic Bacteria in Salt that is Used in Brine Curing of Hides. *J. Electrostat.* **66**(7-8), 388-394, 2008b.
36. Birbir, Y., Dolek, N., Birbir, M., Caglayan, P.; Extermination of Bacteria in Hide-Brine Curing Liquors Using Combined Alternating and Direct Electric Current Applications Plus Bronopol. *Rom. Biotechnol. Lett.* **20**(1), 10123-10133, 2015a.
37. Birbir, Y., Anik, S., Birbir, M., Caglayan, P.; Annihilation of Extremely Halophilic Archaea in Hide Preservation Salt Using Alternating Electric Current. *Johnson Matthey Technol. Rev.* **59**(2), 109-119, 2015b.
38. Birbir, M., Cicek, R., Caglayan, P., Aslan, E.; An Examination of Inactivation Efficacy of NaCl and Boric Acid on Bacteria Isolated from Salted Hides. *JALCA* **108**(5), 171-179, 2013a.
39. Birbir, Y., Dolek, N., Birbir, M.; Effect of a Combined Treatment Using both Direct and Alternating Electric Currents on Hide Bacteria in Hide-Soak Liquor. *J. Electrostat.* **71**(5), 898-904, 2013b.
40. Caglayan, P., Birbir, M., Ogan, A., Ventosa, A., Sánchez-Porro, C., Birbir, Y.; The Effects of Alternating and Direct Electric Currents on Moderately Halophilic Bacteria in Leather Industry. *J. Soc. Leather Technol.Chem.* **100**, 307-313, 2016.
41. Sale, A.J.H., Hamilton, W.A.; Effects of High Electric Fields on Microorganisms: Killing of Bacteria and Yeasts. *Biochim. Biophys. Acta.* **148**, 781-788, 1967.
42. Matsunaga, T., Nakasono, S., Takamuku, T., Burgess, J. G., Nakamura, N., Sode, K.; Disinfection of Drinking Water by using a Novel Electrochemical Reactor Employing Carbon-cloth Electrodes. *Appl. Environ. Microbiol.* **58**, 686-689, 1992.
43. Park, J. C., Lee, M. S., Lee, D. H., Park, B. J., Han, D. W., Uzawa, M., Takatori, K.; Inactivation of Bacteria in Seawater by Low-amperage Electric Current. *Appl. Environ. Microbiol.* **69**, 2405-2408, 2003.
44. Birbir, M., Ilgaz, A.; Isolation and Identification of Bacteria Adversely Affecting Hide and Leather Quality. *J. Soc. Leather Technol.Chem.* **80**, 147-153, 1996.
45. Sánchez-Porro, C., Martín, S., Mellado, E., Ventosa, A.; Diversity of Moderately Halophilic Bacteria Producing Extracellular Hydrolytic Enzymes. *J. Appl. Microbiol.* **94**, 295-300, 2003.
46. Gonzalez, C., Gutierrez, C., Ramirez, C.; *Halobacterium vallismortis* sp. nov. An Amylolytic and Carbohydrate-Metabolizing, Extremely Halophilic Bacterium. *Can. J. Microbiol.* **24**(6), 710-715, 1978.
47. Montalvo-Rodríguez, R., Vreeland, R.H., Oren, A., Kessel, M., Betancourt, C., López-Garriga, J.; *Halogeometricum borinquense* gen. nov., sp. nov., a Novel Halophilic Archaeon from Puerto Rico. *Int. J. Syst. Bacteriol.* **4**, 1305-1312, 1998.
48. QIAamp DNA Mini and Blood Mini Handbook, Sample and Assay Technologies, pp.1-67, 2010.
49. Mellado, E., Nieto, J.J., Ventosa, A.; Phylogenetic Interferences and Taxonomic Consequences of 16S Ribosomal DNA Sequence Comparison of *Chromohalobacter marismortui*, *Volcaniella eurihalina* and *Deleya halophila* and Reclassification of *V. eurihalina* as *Halomonas eurihalina* comb. nov. *Int. J. Syst. Evol. Microbiol.* **45**, 712-716, 1995.
50. Kim, O.S., Cho, Y.J., Lee, K. *et al.*; Introducing EzTaxon-e: A Prokaryotic *16S rRNA*Gene Sequence Database with Phylotypes

that Represent Uncultured Species. *Int. J. Syst. Evol. Microbiol.* **62**, 716, 2012.

51. Limauro, D., Cannio, R., Fiorentino, G., Rossi, M., Bartolucci, S.; Identification and Molecular Characterization of an Endoglucanase Gene, celS, from the Extremely Thermophilic Archaeon *Sulfolobus solfataricus*. *Extremophiles* **5**, 213-219, 2001.
52. Birbir, M., Calli, B., Mertoglu, B., Bardavid, R.E., Oren, A., Ogmen, N.M., Ogan, A.; Extremely Halophilic *Archaea* from Tuz Lake, Türkiye, and the Adjacent Kaldirim and Kayacik Salterns. *World J.Microbiol. Biotechnol.* **23**, 309-316, 2007.
53. Quesada, E., Bejar, V., Valderrama, M. J., Ventosa, A., Ramos-Cormenzana, A.; Isolation and Characterization of Moderately Halophilic Nonmotile Rods from Different Saline Habitats. *Microbiologia* **1**(1-2), 89-96, 1985.
54. Das Murtey, M., Ramasamy, P.; Sample Preparations for Scanning Electron Microscopy-Life Sciences. *Modern Electron Microscopy in Physical and Life Sciences*, pp. 161-185, 2016.
55. Ammar, O.F.; Preparation of Bacteria for Scanning Electron Microscope and Common Reagents Preparation Protocols, 2017. DOI:10.13140/RG.2.2.16802.84160.
56. Glauert, A.M.; Fixation, Dehydration and Embedding of Biological Specimens. North-Holland Publishing Company, 3rd Edition, Amsterdam, The Netherlands, pp.73-122, 1975.
57. Covington, T.; Tanning Chemistry, The Science of Leather, The Royal Society of Chemistry, Cambridge, UK, 2009.
58. Birbir, Y., Molla, S., Birbir, M.; Applying Electric Current to Inactivate Gram-negative Bacteria isolated from Salt-packed-cured Hides. *J. Soc. Leather Technol. Chem.* **97**, 5-10, 2013.

The American Leather Chemists Association

5997 Center Hill Ave. Cincinnati OH 45224 phone: 513.290.2502
Web: leatherchemist.org email: hallks@ucmail.uc.edu

Past Issues of *Journal* Needed

The ALCA office is working to compile a complete collection of issue of *The Journal of the American Chemists Association.* If you or someone you know has copies of these missing issues you would like to donate to ALCA please contact the ALCA office.

Missing issues needed.

1924 - January

1937 - January and December

1939 - January, March and April

1940 - January

1946 - February

Design credit: Ana Del Rio Mullarkey, People's Choice Award Winner & Joint Overall, 2023 International Student Design Competition

In association with:

ARTS THREAD

REAL LEATHER. STAY DIFFERENT.

2024

INTERNATIONAL STUDENT DESIGN COMPETITION

CALL FOR ENTRIES

CLOTHING | FOOTWEAR | ACCESSORIES

Have you got what it takes to be RLSD's next top International designer? Your College thinks you do! Real Leather. Stay Different. is on a mission to find the best in fresh, free-thinking fashion talent, from around the globe. Working with leather, the competition is open to those who value individuality, promote slow style and love designing with natural materials that will last a lifetime, for a more sustainable future in fashion. Winners will be invited to attend the International final event (travel and accommodation expenses covered by the organisers). With a top judging panel, and prizes including professional production of your design, RLSD trophy, certificate and coffee table book including your winning entry, and inclusion in the RLSD capsule collection which will showcase around the globe, entry is a must for your student portfolio - and winning the kick-start to a great career.

TO ENTER VISIT: **rlsd.internationaldesigncomp.com**
ENTRIES CLOSE: **30/06/2024**
chooserealleather.com

Lifelines

Jaffrin Benseelia holds a Masters Degree in Footwear Engineering and Management, from Anna University, Chennai. She completed her undergraduate degree in Biomedical Engineering and is currently working as Assistant Professor in a Private College.

S. Chris Felshia holds a Doctoral degree in Microbial Biotechnology. Devoted to research in pollutants management using selective microbial species and formulation studies on effective management of microbes. Published more than seven articles in reputed journals. Received First prize for AWSAR AUGMENTATIVE WRITING and won 1 L cash prize. Received Best paper presentation in National and International conferences and symposia.

Victor John Sundar obtained his Doctorate in Technology from Anna University, India. He has made significant contributions towards Process & Product Innovations, Technology Dissemination, Human Resource Development, Standards Development, Product Evaluation and Advisory Consultancy for leather and chemical sectors since joining CSIR-CLRI in 1993. He has developed a number of process technologies aimed at resource management and waste minimization resulting in more than 30 patents and 150 research papers. He has led many technology implementation teams for cleaner process techniques and for modernization of tanneries. His current areas of research include development of cleaner technologies, water management and solid waste management in leather processing. He is recipient of National and International Awards and Honorary faculty of Anna University, India.

A. Gnanamani received her Doctoral degree in Science and is involved in challenging research activities in microbiology, biotechnology, environmental issues, biological material for health care and development of analytical tools. She has published more than 200 research articles with more than 5200 citations with i10 index 109 and h-index 37. She has filed more than 10 patents and three patents have been transferred to the industries. Her research team is involved in the development of innovative materials for health care and diagnosis. She is a recipient of prestigious awards which includes: Tamil Nadu Scientist Award, TATA innovation Fellowship award, DBT-OVERSEAS AWARD, DBT –CREST AWARD, IIGP (India Innovative Growth Programme) Gold medal, Best women scientist award, Scientific Excellence award and SKOCH order of merit award.

Cheng Haiming, see JALCA 131, **109,** 2014

Zhou Jin is now an associate professor in the Department of Fashion Design of Garment and Leather Products, Sichuan University, China.

Shi Haonan is now a graduate student in the Department of Biomass and Leather Engineering, Sichuan University, China. He received his Bachelor's degree in engineering from Sichuan University in 2020. His research field is related to the comfort of leather products.

Guang Jin entered the College of Mechanical & Electrical Engineering at Shaanxi University of Science & Technology in Xi 'an, China in 2021 to pursue a master's degree. His main research interests are leather grasping robots and computer vision.

Gongchang Ren received his Ph.D. from Xi 'an Jiaotong University in 2006. He is now a professor and doctoral supervisor at the College of Mechanical & Electrical Engineering at Shaanxi University of Science & Technology in Xi 'an, China. Mainly engaged in product innovation design, service robot technology, mechanical and electrical equipment status monitoring and other aspects of research work.

Yuan Huan began his doctoral studies in 2020 at the College of Mechanical & Electrical Engineering at Shaanxi University of Science & Technology in Xi ‘an, China. His research interests lie in the theory of product innovation and robotics-related technologies.

Jiangong Sun began his doctoral studies in 2021 at the College of Mechanical & Electrical Engineering at Shaanxi University of Science & Technology in Xi ‘an, China. His primary research focus is on robotics-related technologies.

Senanur Kose graduated from the Biology Department of Kocaeli University Faculty of Arts and Sciences in 2019. She received her Master’s Degree in the Department of Biology at Marmara University, Institute of Pure and Applied Sciences. Her research areas include skin microbiology, antimicrobial agents, bacterial enzymes and haloversatile bacteria.

Pinar Yilmaz graduated from the Biology Department, Atatürk Faculty of Education, Marmara University. She received her MSc and PhD Degrees in Biology from the Institute of Pure and Applied Sciences, Marmara University. She was an Erasmus student in the Department of Microbiology and Parasitology, Faculty of Pharmacy, Sevilla University, Spain from 2008–2009. She has been working at the Division of Plant Diseases and Microbiology, Marmara University since 2011. Her research interests are moderately halophilic bacteria, extremely halophilic archaea, antimicrobial agents, hide microbiology and electric current applications on microorganisms.

Meral Birbir graduated from the Biology Department, Atatürk Faculty of Education, Marmara University. She received her MSc and PhD Degrees in Biology (especially microbiology) from the Institute of Pure and Applied Sciences, Marmara University. Professor Birbir has been working in the Biology Department of Marmara University since 1985. She was a research scientist at the Department of Pathology and Microbiology, Veterinary Medical School, Purdue University, USA (1990) and Hides and Leather Department of the US Department of Agriculture (1992–1993). Her research interests are industrial enzymes, halophilic microorganisms, hide and skin microbiology, antimicrobial agents, antibiotic resistance, electric current applications on microorganisms and bacterial, archaeal and fungal communities in hypersaline environments.

Yasar Birbir received his BSc Degree from Gazi University, Türkiye, and MSc and PhD Degrees in Electrical Education from Marmara University. He has been working at Marmara University since 1983. He attended the World Bank Industrial Training Project at Indiana and Purdue Universities, USA (1989–1990). He worked as a visiting research scientist at the Electrical and Computer Engineering Department of Drexel University, USA (1992–1993). He has been working as a Professor at the Technology Faculty, Department of Electrical Engineering, Marmara University. His current interests are power electronic converters and drivers, electromagnetic filtering processes in industry and applications of electric currents for inactivation of different microorganisms.

INDEX TO ADVERTISERS

REMINDER:
Presentations are due May 1st, 2024

CALL FOR PAPERS

FOR THE 118th ANNUAL CONVENTION OF THE AMERICAN LEATHER CHEMISTS ASSOCIATION

Hershey Lodge, Hershey Pennsylvania
May 21–24, 2024

If you have submitted an abstract for presentation of your recent research to present at the annual ALCA convention at the Hershey Lodge, Hershey Pennsylvania, May 21–24, 2024, the full presentation is due May 1, 2024. Please contact the Technical Program Chair or the Editor if you have any questions.

Abstracts are due by March 1, 2024
Full Presentations are due by May 1, 2024

They are to be submitted by e-mail to the
ALCA Vice-President and Chair of the Technical Program:

John Rodden
Union Specialties, Inc.
3 Malcom Hoyt Dr.
Newburyport, MA 01950
E-mail: johnrodden@unionspecialtiesinc.com

The **Abstract** should begin with the title in capital letters, followed by the authors' names. An asterisk should denote the name of the speaker, and contact information should be provided that includes an e-mail address. The abstract should be no longer than 300 English words, and in the Microsoft Word format.

Full Presentations at the convention will be limited to 25 minutes. In accordance with the Association Bylaws, all presentations are considered for publication by *The Journal of the American Leather Chemists Association.* They are not to be published elsewhere, other than in abstract form, without permission of the *Journal* Editor. For further paper preparation guidelines please refer to the *JALCA* Publication Policy on our website: leatherchemists.org

Full Presentations are to be submitted by e-mail to the *JALCA* editor:

Steven D. Lange, *Journal* Editor
The American Leather Chemists Association
E-mail: jalcaeditor@gmail.com
Mobile Phone (814) 414-5689

118th ALCA ANNUAL CONVENTION May 21 – 24, 2024 Hershey Lodge, Hershey PA

Featuring the 63nd John Arthur Wilson Memorial Lecture

***By* Panos Mytaros**
Chief Executive Officer
ECCO

Tentative Schedule

Tuesday, May 21
Golf Tournament, Opening Reception and Dinner

Wednesday, May 22
John Arthur Wilson Memorial Lecture All Day
Technical Sessions, Fun Run, Reception and Dinner

Thursday, May 23
All Day Technical Sessions, Annual Business Meeting
Activities Awards Luncheon
Social Hour, Banquet Dinner

Visit us at www.leatherchemists.org for full details under Annual Convention as they become available